Magnetic Small-Angle Neutron Scattering: A Probe for Mesoscale Magnetism Analysis

Andreas Michels

Department of Physics and Materials Science, University of Luxembourg









Acknowledgements

- Mathias Bersweiler, Ivan Titov, Venus Rai, Elizabeth Jefremovas, Evelyn Pratami Sinaga, Michael Adams, Stefan Liscak (University of Luxembourg)
- Joachim Kohlbrecher (PSI), Dirk Honecker & Diego Alba Venero (ISIS), Sebastian Mühlbauer (TUM), Nina-Juliane Steinke (ILL)
- María del Puerto Morales (ICMM-CSIC, Madrid)
- Luis F. Barquín (U Cantabria)
- Hamid Kachkachi (U Perpignan)
- Konstantin Metlov (Donetsk)
- Sergey Erokhin, Dmitry Berkov (General Numerics Research Lab, Jena)





Outline

- > The very basics of magnetic neutron scattering
- **✓** Properties of the neutron
- **✓** Basic interactions, Born approximation, magnetic scattering cross section...
- > Magnetic Small-Angle Neutron Scattering (SANS)
- ✓ Origin of magnetic SANS
- ✓ Analytical SANS theory
- **✓** Analysis of magnetic microstructure
- ✓ Real-space analysis
- > Selected Examples
- **✓** Impact of DMI: Symmetry breaking at defect sites
- ✓ Scaling in magnetic SANS
- **✓** Signatures of hopfions
- Conclusion

Basic properties of the neutron

- Neutron is an elementary particle, which has been discovered by James Chadwick in 1932 (Nobel Prize 1935)
- mass m = 1.675×10^{-27} kg (-> de Broglie wavelength in Å regime; allows to study static and dynamic structure of matter)
- spin angular momentum of $S=\pm \frac{1}{2}\hbar$ and associated magnetic dipole moment of $\mu=$ 1.913 μ_N (-> allows to probe magnetism)
- zero net electrical charge (-> weak interaction; interpretation of scattering data in terms of Born approximation)
- average lifetime of a free neutron is ~ 886 seconds (long enough)
- → neutrons are extremely attractive for research purposes, in particular, for investigating the structure and dynamics of matter on a wide range of length and time scales

Classification of research neutrons

	Energy [meV]	Temperature [K]	Wavelength [Å]	Velocity [m/s]
hot neutrons	100-500	1200-6000	1-0.4	4000-10000
thermal neutrons	10-100	120 - 1200	3-1	1000-4000
cold neutrons	0.1-10	1-120	30-3	130-1300

H. Schober, J. Neutron Research <u>17</u>, 109 (2014).

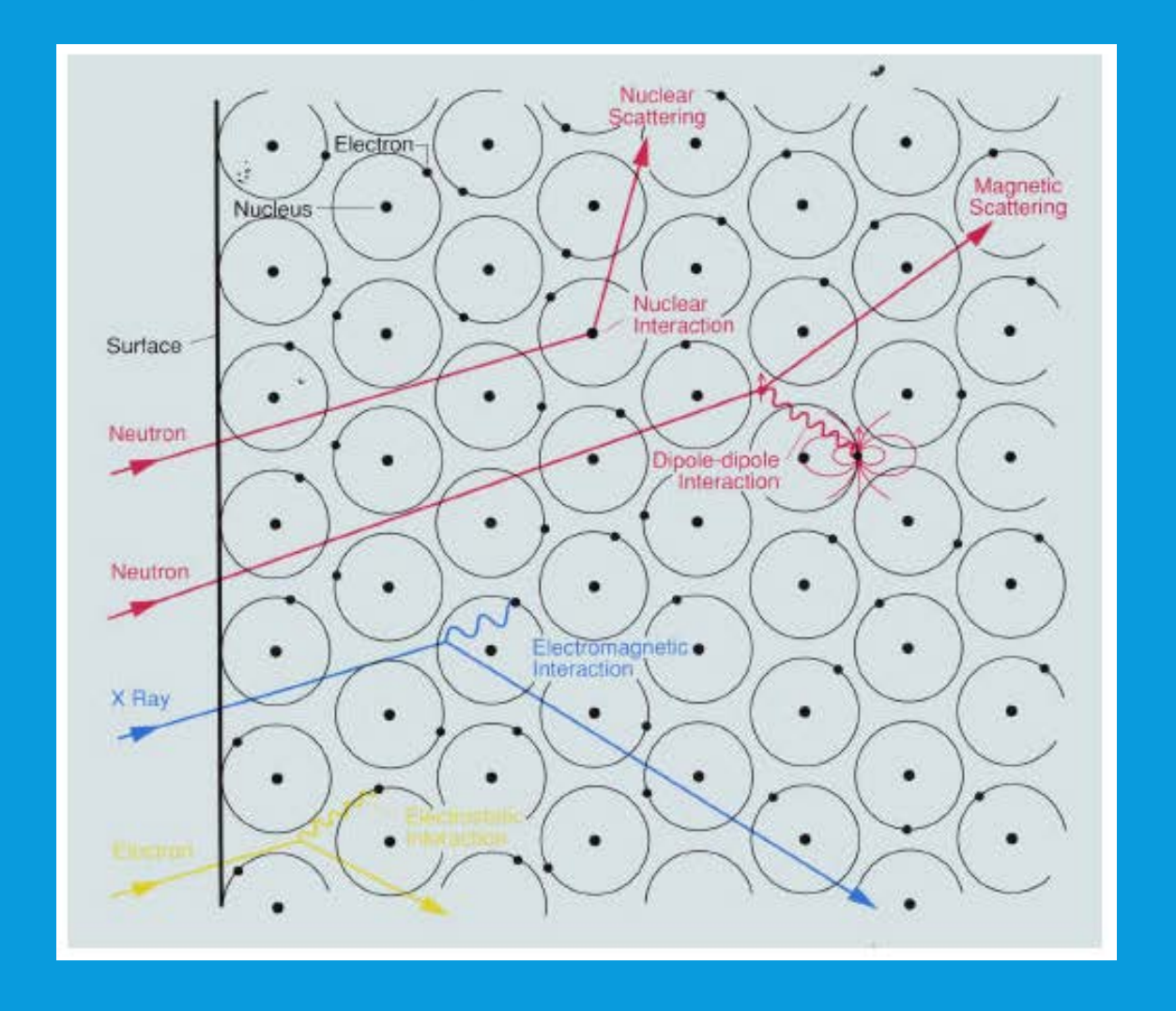
$$E = kT = \frac{1}{2} m v^{2}$$

$$\lambda = \frac{h}{(mv)}$$

$$k = \frac{2\pi}{\lambda}$$

$$\mathbf{p} = \hbar \mathbf{k}$$

Neutron-Matter Interaction Mechanisms



R. Pynn, in *Neutron Scattering: A Primer*, Los
Alamos Science (1990).

- **■** Neutrons interact with atomic nuclei via very short-range (~ fm) forces
- □ Neutrons also interact with unpaired electrons via a magnetic dipole interaction

The cross section: Born approximation

- In general we consider the scattering process of neutrons by a sample during which the sample state changes from s_0 to s_1 (e.g., via the excitation or annihilation of a phonon or magnon) while the state of neutron changes from k_0 , σ_0 to k_1 , σ_1
- For <u>elastic scattering</u> ($s_0 = s_1$) and ignoring the spin degree of freedom of the neutron (σ), the cross section is given by (only direction of neutron beam changes)

$$\frac{d\Sigma}{d\Omega} = \frac{1}{V} \frac{1}{\Phi} \frac{1}{d\Omega} \sum_{\mathbf{k}_1 \text{ in } d\Omega}^{\mathbf{transition rate}} W_{\mathbf{k}_0 \to \mathbf{k}_1}$$

$$\sum_{\mathbf{k}_1 \text{ in } d\Omega} W_{\mathbf{k}_0 \to \mathbf{k}_1} = \frac{2\pi}{\hbar} \rho_{\mathbf{k}_1} \left| \langle \mathbf{k}_1 | V_{\text{int}} | \mathbf{k}_0 \rangle \right|^2$$
Fermis Golden Rule

- where V_{int} denotes the neutron-matter interaction potential (to be specified)
- Born approximation: incoming and outgoing neutron waves are in a plane-wave state
- In Born approximation, the matrix element reduces to the Fourier transform of V_{int}

Basic interactions of research neutrons with matter

Modeled by Fermi Pseudo potential; very short range; gives correct result in first Born approximation; Neutron wavelength (a few Å) >> size of the nucleus -> isotropic s-wave scattering

Nuclear
$$\sum_{\mathbf{k}_1 \text{ in } d\Omega} W_{\mathbf{k}_0 \to \mathbf{k}_1} = \frac{2\pi}{\hbar} \rho_{\mathbf{k}_1} \left| \langle \mathbf{k}_1 | V_{\text{int}} | \mathbf{k}_0 \rangle \right|^2$$
 Scattering

$$V_{\mathrm{int}}^{\mathrm{nuc}}(\mathbf{r}) = \frac{2\pi\hbar^2}{m_{\mathrm{n}}} b\delta(\mathbf{r})$$

$$b = b' - ib''$$

nuclear scattering length (bound); $b \sim a$ few fm = 10^{-15} m b" describes absorption (³He, B, Cd, Gd); for most materials b" << b'

$$\frac{d\sigma_{\text{nuc}}}{d\Omega}(\mathbf{q}) = \left| \sum_{m=1}^{N} b_m e^{-i\mathbf{q}\mathbf{r}_m} \right|^2 = \sum_{m,n} b_m b_n^* e^{-i\mathbf{q}(\mathbf{r}_m - \mathbf{r}_n)}$$

Basic interactions of research neutrons with matter

 \bullet The magnetic moment of the neutron μ_n interacts with the magnetic field B, which is produced by the spin (B_S) and orbital motion (B_L) of the electrons

Scattering

Magnetic
$$\sum_{\mathbf{k}_1 \text{ in } d\Omega} W_{\mathbf{k}_0 \to \mathbf{k}_1} = \frac{2\pi}{\hbar} \rho_{\mathbf{k}_1} \left| \langle \mathbf{k}_1 | V_{\text{int}} | \mathbf{k}_0 \rangle \right|^2$$

$$V_{
m int}^{
m mag}(\mathbf{r}) = -oldsymbol{\mu}_{
m n} \cdot \mathbf{B}(\mathbf{r})$$

$$\mathbf{B} = \mathbf{B}_{\mathrm{S}} + \mathbf{B}_{\mathrm{L}} = \frac{\mu_{0}}{4\pi} \left(\nabla \times \frac{\boldsymbol{\mu}_{\mathrm{e}} \times \mathbf{r}}{r^{3}} - \frac{2\mu_{\mathrm{B}}}{\hbar} \frac{\mathbf{p} \times \mathbf{r}}{r^{3}} \right)$$

Dipole-dipole interaction (long-range and anisotropic)

Elastic Magnetic (Small-Angle) Neutron Scattering

$$\sum_{\mathbf{k}_1 \text{ in } d\Omega} W_{\mathbf{k}_0 \to \mathbf{k}_1} = \frac{2\pi}{\hbar} \rho_{\mathbf{k}_1} \left| \langle \mathbf{k}_1 | V_{\text{int}} | \mathbf{k}_0 \rangle \right|^2 \quad V_{\text{int}}^{\text{mag}}(\mathbf{r}) = -\boldsymbol{\mu}_{\text{n}} \cdot \mathbf{B}(\mathbf{r})$$

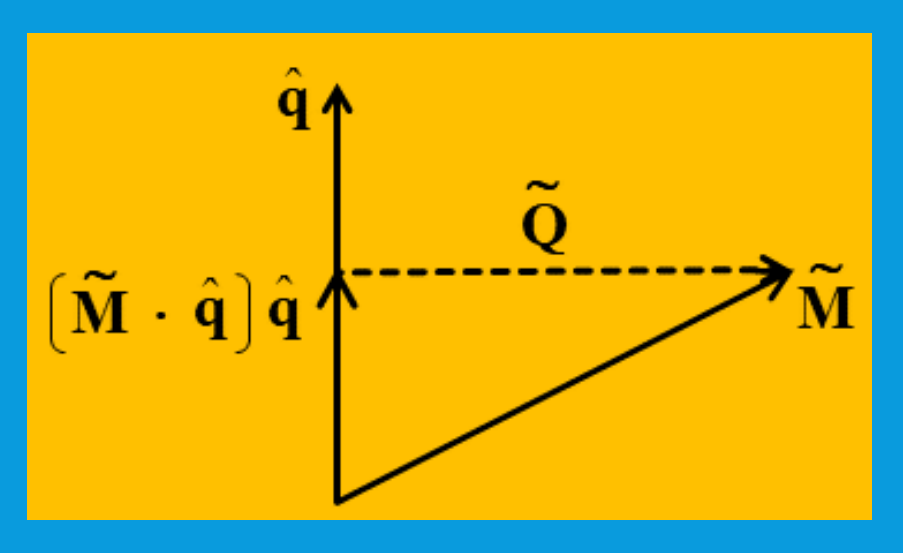
$$\mathbf{M}(\mathbf{r}) = \frac{1}{(2\pi)^{3/2}} \int_V \widetilde{\mathbf{M}}(\mathbf{q}) e^{i\mathbf{q}\mathbf{r}} d^3q \ \widetilde{\mathbf{M}}(\mathbf{q}) = \frac{1}{(2\pi)^{3/2}} \int_V \mathbf{M}(\mathbf{r}) e^{-i\mathbf{q}\mathbf{r}} d^3r$$

$$\begin{split} \frac{d\Sigma_{\mathrm{M}}}{d\Omega}(\mathbf{q}) &= \frac{1}{V}b_{\mathrm{H}}^{2} \left| \int_{V} \mathbf{Q}(\mathbf{r})e^{-i\mathbf{q}\mathbf{r}}d^{3}r \right|^{2} = \frac{8\pi^{3}}{V}b_{\mathrm{H}}^{2} |\widetilde{\mathbf{Q}}|^{2} \\ &= \frac{8\pi^{3}}{V}b_{\mathrm{H}}^{2} \left| \widehat{\mathbf{q}} \times \left(\widetilde{\mathbf{M}}(\mathbf{q}) \times \widehat{\mathbf{q}} \right) \right|^{2} \\ &= \frac{8\pi^{3}}{V}b_{\mathrm{H}}^{2} \sum_{\alpha,\beta} \left(\delta_{\alpha\beta} - \widehat{q}_{\alpha}\widehat{q}_{\beta} \right) \widetilde{M}_{\alpha}\widetilde{M}_{\beta} \end{split}$$

$$b_{\rm m} = \frac{\gamma_{\rm n} r_{\rm e}}{2} \frac{\mu_{\rm a}}{\mu_{\rm B}} f(\mathbf{q}) \approx 2.70 \times 10^{-15} \,\mathrm{m} \frac{\mu_{\rm a}}{\mu_{\rm B}} f(\mathbf{q}) \approx b_{\rm H} \mu_{\rm a} \qquad b_{\rm H} = 2.70 \times 10^{-15} \,\mathrm{m} \,\mu_{\rm B}^{-1} = 2.91 \times 10^8 \,\mathrm{A}^{-1} \mathrm{m}^{-1}$$

Elastic Magnetic (Small-Angle) Neutron Scattering

$$\widetilde{\mathbf{Q}}_i = \hat{\mathbf{q}} \times (\hat{\mathbf{m}}_i \times \hat{\mathbf{q}}) = \hat{\mathbf{m}}_i - \hat{\mathbf{q}}(\hat{\mathbf{q}} \cdot \hat{\mathbf{m}}_i)$$



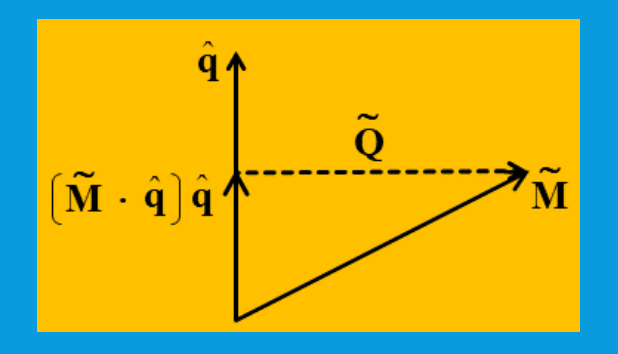
- > is called the magnetic interaction or Halpern-Johnson vector
- Embodies anisotropic character of magnetic neutron scattering due to dipole-dipole interaction
- > Only the component of M which is perpendicular to the scattering vector q contributes to the magnetic neutron scattering cross section

Elastic Magnetic (Small-Angle) Neutron Scattering

For a single magnetic domain

$$\widetilde{\mathbf{Q}}_i = \hat{\mathbf{q}} \times (\hat{\mathbf{m}}_i \times \hat{\mathbf{q}}) = \hat{\mathbf{m}}_i - \hat{\mathbf{q}}(\hat{\mathbf{q}} \cdot \hat{\mathbf{m}}_i)$$
 $|\widetilde{\mathbf{Q}}_i|^2 \propto \sin^2 \alpha_i$

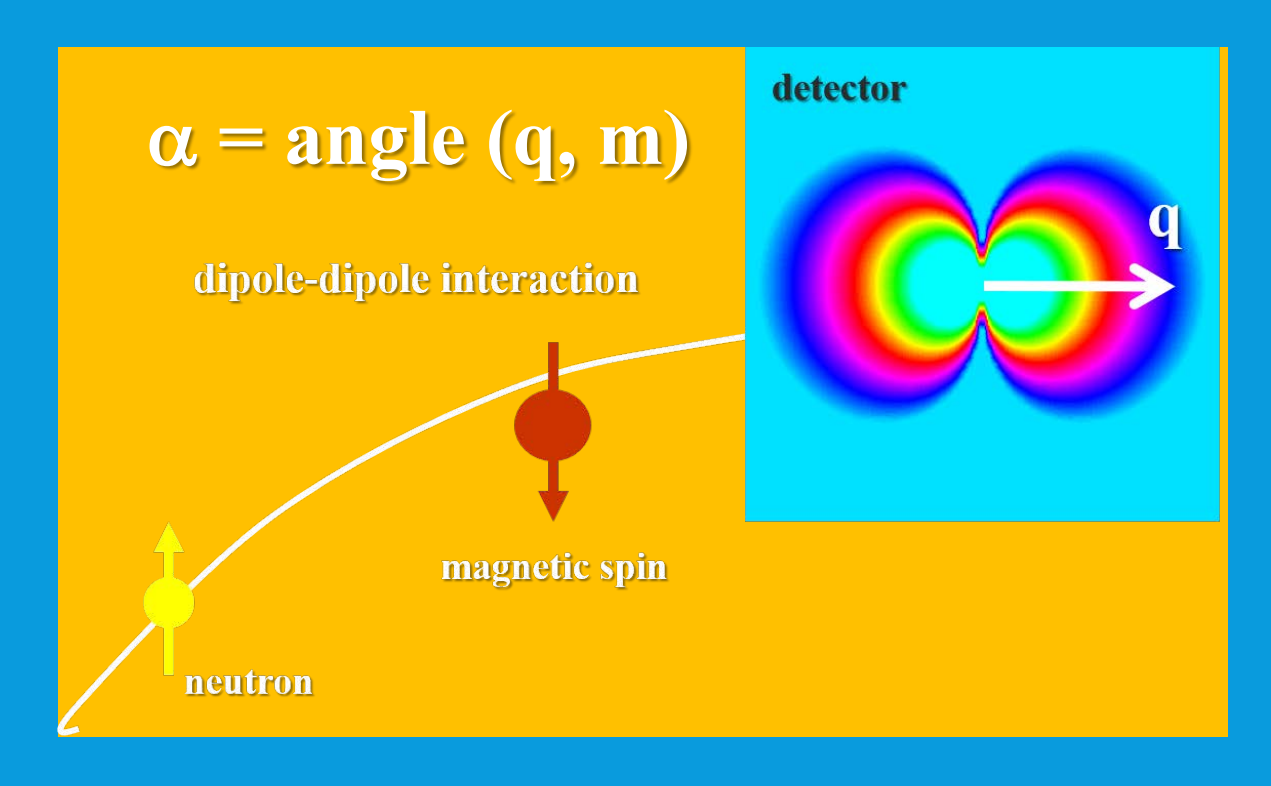
$$|\widetilde{\mathbf{Q}}_i|^2 \propto \sin^2 \alpha_i$$



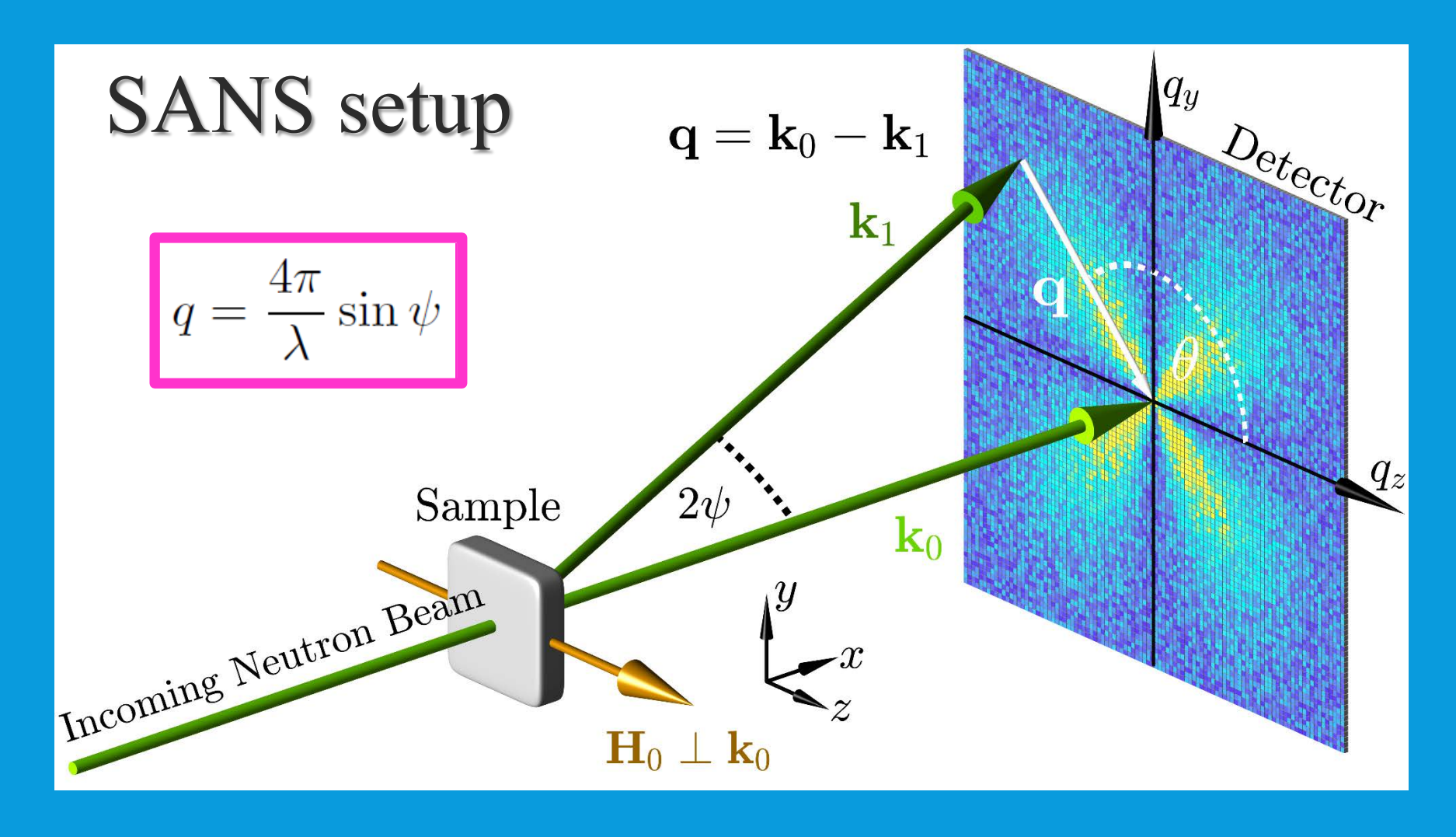
for unpolarized neutrons

$$\frac{d\Sigma_{\text{tot}}}{d\Omega} = \frac{d\Sigma_{\text{nuc}}}{d\Omega} + \frac{d\Sigma_{\text{mag}}}{d\Omega}$$
$$= \frac{d\Sigma_{\text{nuc}}}{d\Omega} + \widetilde{M}_s^2(q)\sin^2\alpha$$

$$\frac{d\Sigma_{\text{tot}}}{d\Omega} = \frac{d\Sigma_{\text{nuc}}}{d\Omega} \quad (\alpha = 0^{\circ})$$



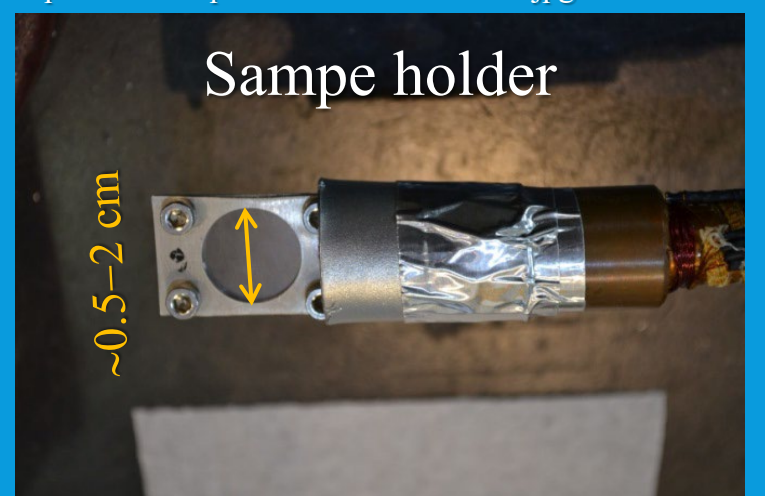
Measurement of unpolarized cross section in saturated single-domain state allows the separation of nuclear and magnetic scattering



- ➤ SANS probes nuclear (structural) and <u>magnetic</u> inhomogeneities in the <u>bulk</u> and on the <u>mesoscale</u> (~ 1 nm up to 1000 nm)
- $\ge 2 \psi < 10^{\circ}$ small angles; $5 \text{Å} < \lambda < 20 \text{Å} \to 0.001 \text{ nm}^{-1} < q < 1 \text{ nm}^{-1}$



https://kur.web.psi.ch/sans1/sans/sans10.jpg



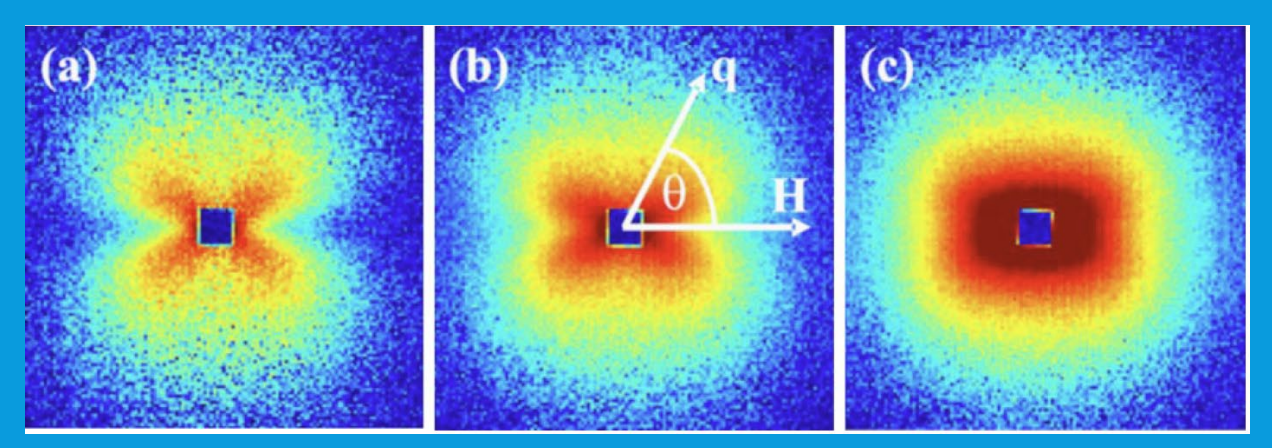


> SANS beamtime is given based on a peer-review process; 1-2 pages proposal; 6-12 month lead time

Richness of magnetic SANS

plethora of angular anisotropies and complex interactions

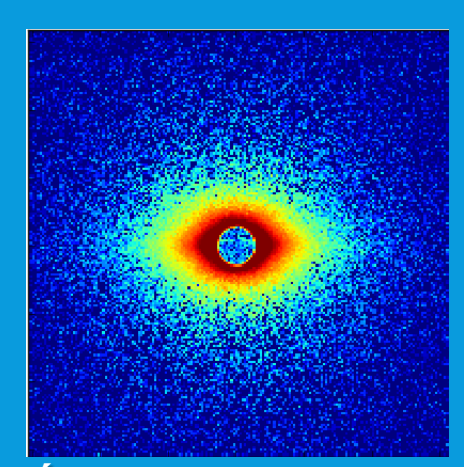
NANOPERM



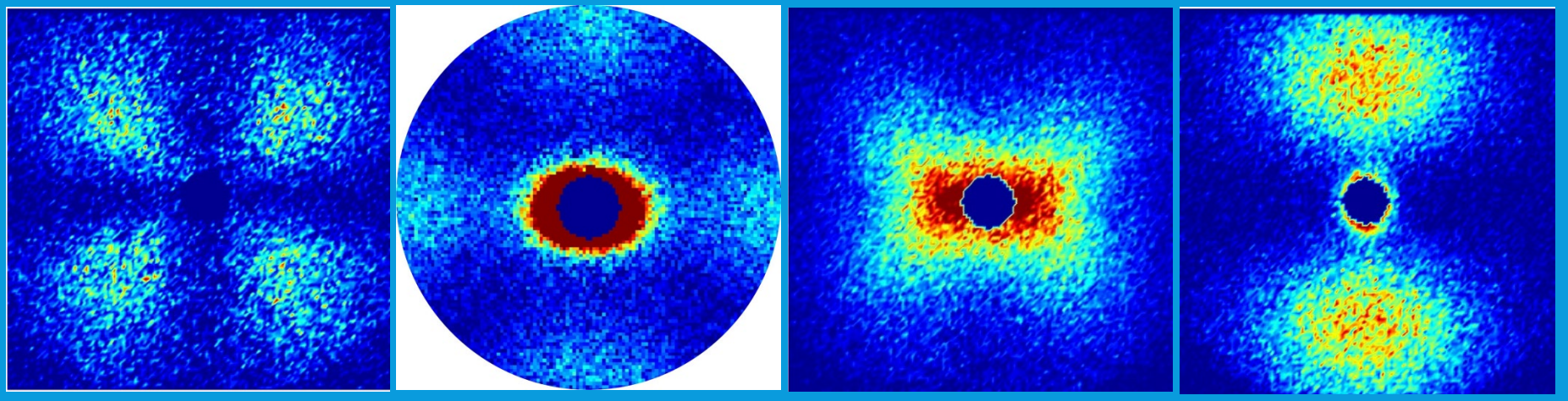
A. Michels et al., PRB 74, 134407 (2006).

Fe-based alloys

Nd-Fe-B

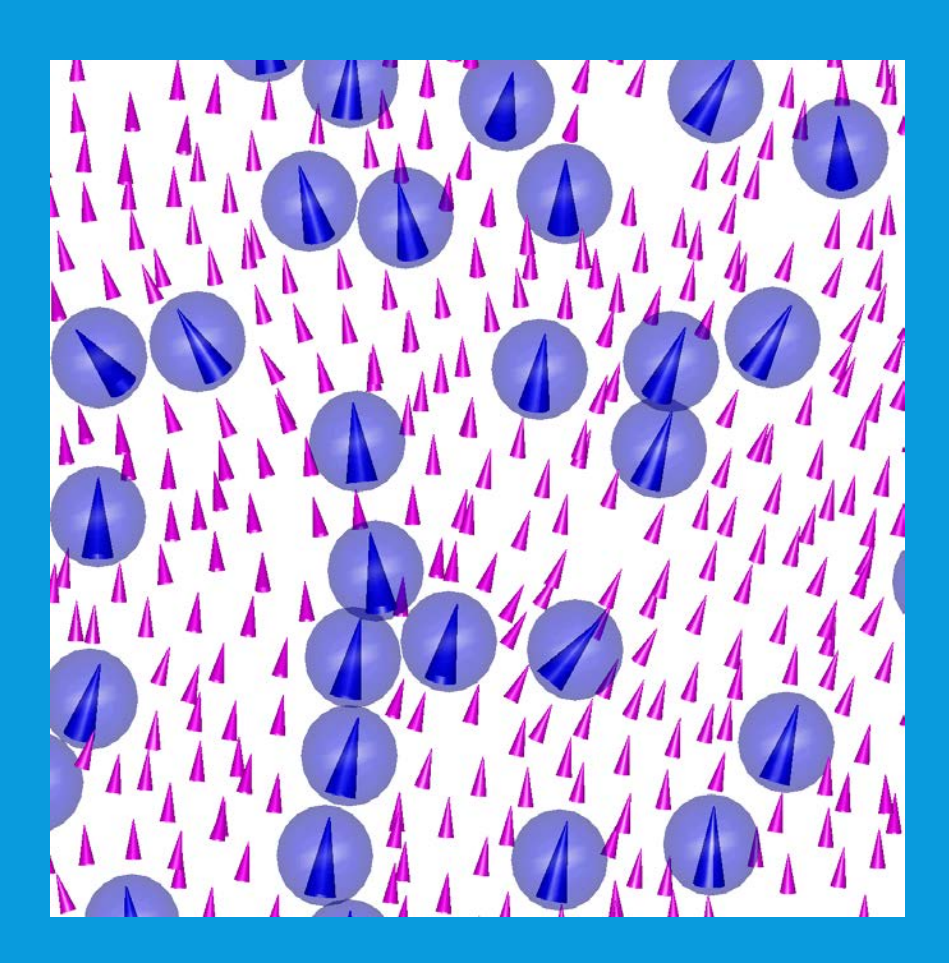


É.A. Périgo *et al.*, NJP <u>16</u>, 123031 (2014).



D. Honecker *et al.*, EPJ B <u>76</u>, 209 (2010).

➤ Magnetic SANS can be described within a continuum approach: relevant quantity is the magnetization vector field



$$\mathbf{M} = \mathbf{M}(\mathbf{r}) = \left\{ \begin{array}{l} M_x(x, y, z) \\ M_y(x, y, z) \\ M_z(x, y, z) \end{array} \right\}$$

- ✓ SANS wavelength above Bragg cutoff for many crystalline materials → no information on discrete atomic structure of matter
- ✓ Discrete atomistic or even purely quantum mechanical calculations limited to very small systems

S. Erokhin, General Numerics Research Lab

Elastic Magnetic Neutron Scattering Cross Section

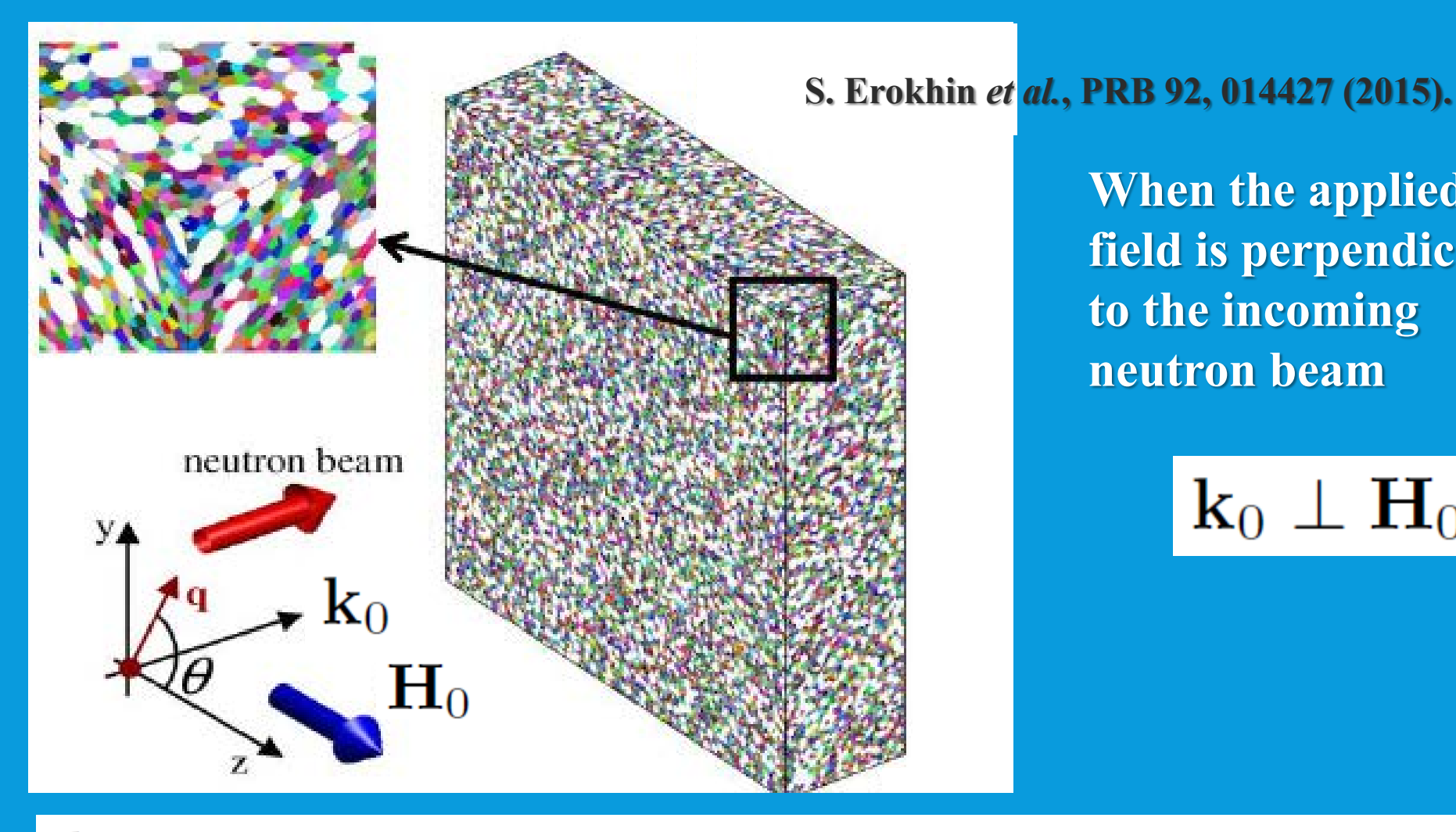
$$\begin{split} \frac{d\Sigma_{\mathbf{M}}}{d\Omega}(\mathbf{q}) &= \frac{1}{V}b_{\mathbf{H}}^2 \left| \int_V \mathbf{Q}(\mathbf{r})e^{-i\mathbf{q}\mathbf{r}}d^3r \right|^2 = \frac{8\pi^3}{V}b_{\mathbf{H}}^2 |\widetilde{\mathbf{Q}}|^2 \\ &= \frac{8\pi^3}{V}b_{\mathbf{H}}^2 \left| \widehat{\mathbf{q}} \times \left(\widetilde{\mathbf{M}}(\mathbf{q}) \times \widehat{\mathbf{q}} \right) \right|^2 \begin{array}{c} \mathbf{Halpern-Johnson} \\ \mathbf{vector} \end{array} \\ &= \frac{8\pi^3}{V}b_{\mathbf{H}}^2 \sum_{\alpha,\beta} \left(\delta_{\alpha\beta} - \widehat{q}_{\alpha}\widehat{q}_{\beta} \right) \widetilde{M}_{\alpha} \widetilde{M}_{\beta} \end{split}$$

$$\mathbf{M}(\mathbf{r}) = \frac{1}{(2\pi)^{3/2}} \int_{V} \widetilde{\mathbf{M}}(\mathbf{q}) e^{i\mathbf{q}\mathbf{r}} d^{3}q \quad \widetilde{\mathbf{M}}(\mathbf{q}) = \frac{1}{(2\pi)^{3/2}} \int_{V} \mathbf{M}(\mathbf{r}) e^{-i\mathbf{q}\mathbf{r}} d^{3}r$$

Central quantity is the Fourier transform of M

$$\widetilde{M}_{x,y,z} = \widetilde{M}_{x,y,z}(q,\theta,H,A,D,M_s,K,\lambda,f(R),\ldots)$$

Elastic Magnetic Neutron Scattering Cross Section



When the applied field is perpendicular to the incoming neutron beam

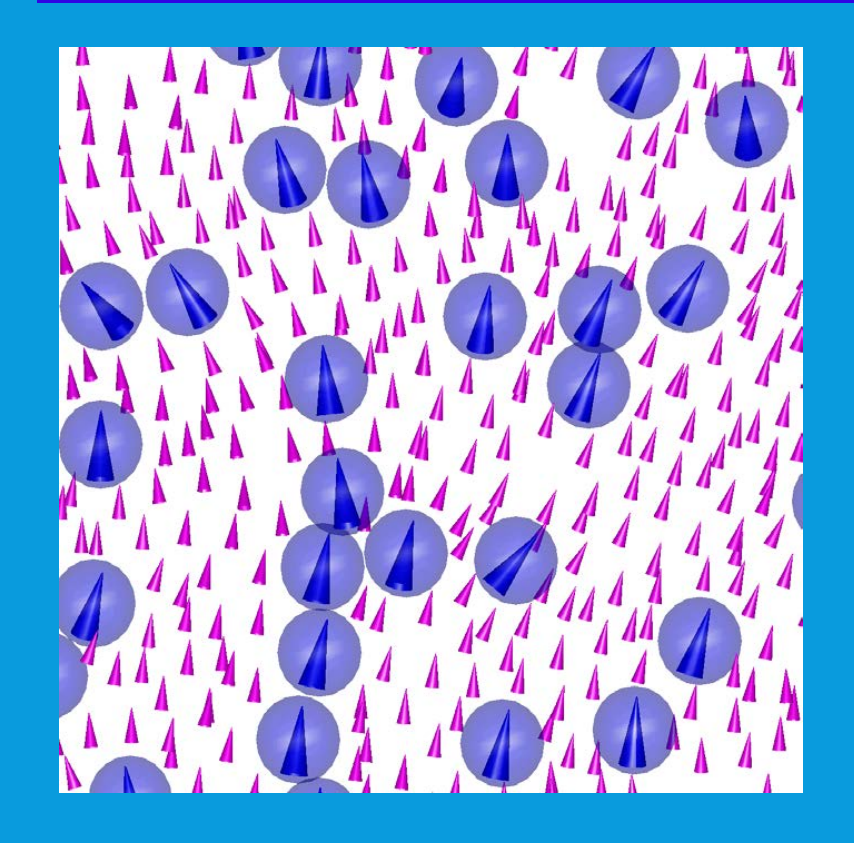
 $\mathbf{k}_0 \perp \mathbf{H}_0$

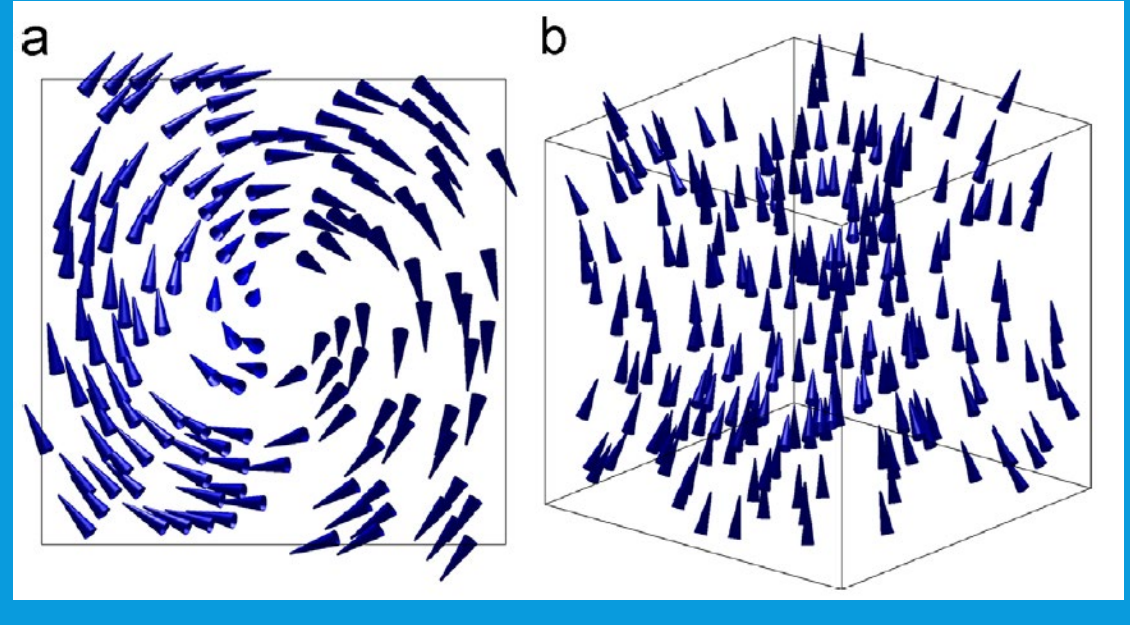
$$\frac{d\Sigma_{\rm M}}{d\Omega} \sim |\widetilde{M}_x|^2 + |\widetilde{M}_y|^2 \cos^2 \theta + |\widetilde{M}_z|^2 \sin^2 \theta - (\widetilde{M}_y \widetilde{M}_z^* + \widetilde{M}_y^* \widetilde{M}_z) \sin \theta \cos \theta$$

- > Origin of diffuse magnetic SANS?
- ➤ Why do we observe a magnetic SANS signal?

Origin of magnetic SANS

➤ Magnetic SANS is due to nanoscale spatial variations in the <u>magnitude</u> and/or <u>orientation</u> of M(r)





S. Erokhin *et al.*, PRB 85, 024410 (2012).

What is the origin of magnetic SANS?

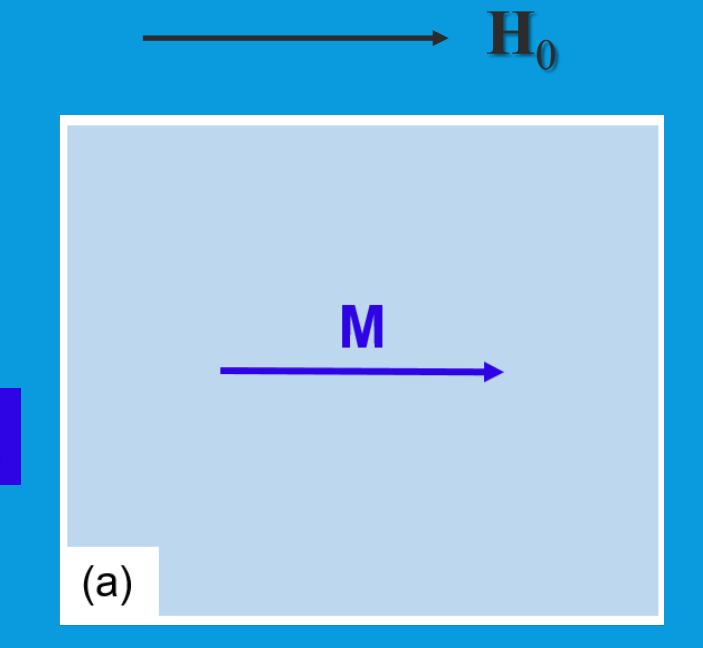
➤ Magnetic SANS is due to nanoscale spatial variations in the <u>magnitude</u> and/or <u>orientation</u> of the magnetization vector field



$$\rightarrow$$
 M = {0, 0, M_s }, where M_s = constant

$$\frac{d\Sigma_{\mathrm{M}}^{\mathrm{sat}}}{d\Omega} \propto |\delta(\mathbf{q})|^2$$

no magnetic SANS signal

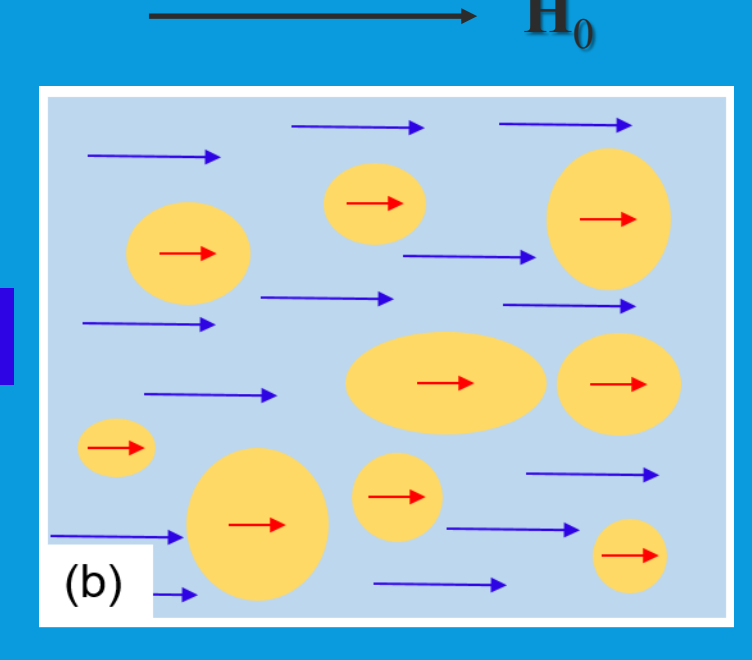


What is the origin of magnetic SANS?

(b) saturated inhomogeneous ferromagnet

$$\to M = \{0, 0, M_s\}, \text{ where } M_s = M_s(x, y, z)$$

$$rac{d\Sigma_{
m M}^{
m sat}}{d\Omega} \propto |\widetilde{M}_s({f q})|^2 egin{array}{c} {
m magnetic SANS \ signal \ } \end{array}$$



$$\widetilde{M}_s(\mathbf{q})$$
 = Fourier transform of $M_s(\mathbf{r})$

magnetic scattering contrast $(\Delta M)^2 = (---)^2 = (M_s^p - M_s^m)^2$

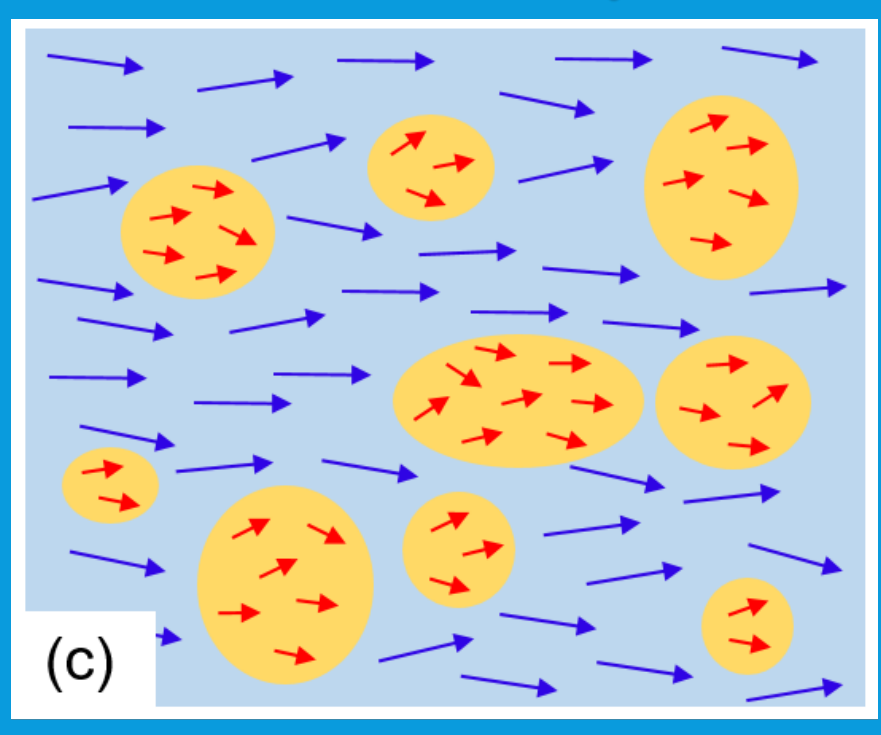
- > For case (b), analysis of magnetic SANS cross section provides information on the size (distribution) and shape (form factor), on the contrast $(\Delta M)^2$, and on the interaction potential between "particles" and "matrix" (structure factor)
- \triangleright However, not really magnetic SANS, scalar function $M_s(r)$, can be mapped onto nuclear SANS problem

What is the origin of magnetic SANS?

(c) nonsaturated inhomogeneous ferromagnet

$$\rightarrow$$
 M = { $M_x(\mathbf{r}), M_y(\mathbf{r}), M_z(\mathbf{r})$ }

$$\longrightarrow$$
 \mathbf{H}_0

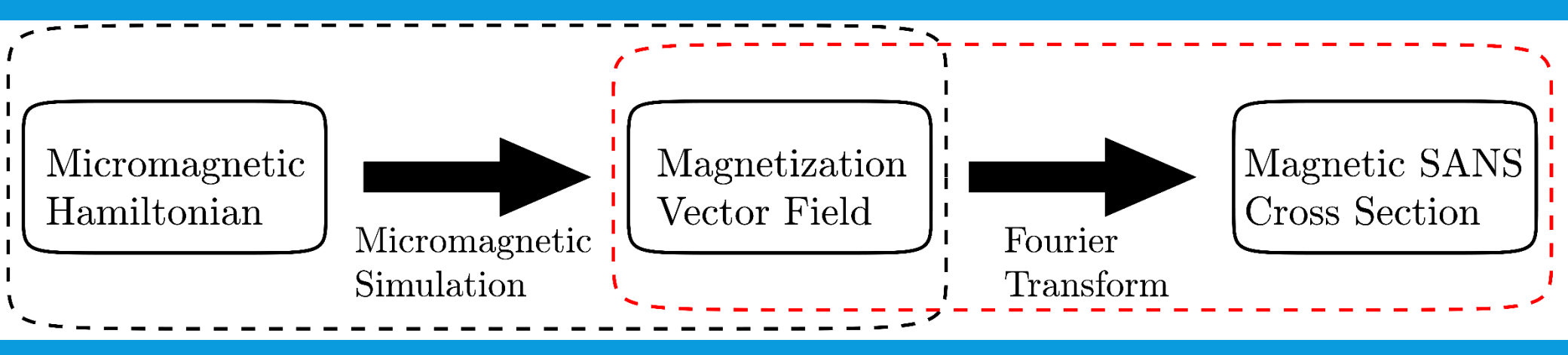


- ✓ In the general case (iii), all three magnetization components determine the magnetic SANS cross section
- → static micromagnetism

 $\mathbf{k}_0 \perp \mathbf{H}_0$

$$\frac{d\Sigma_{\rm M}}{d\Omega} \sim |\widetilde{M}_x|^2 + |\widetilde{M}_y|^2 \cos^2 \theta + |\widetilde{M}_z|^2 \sin^2 \theta - (\widetilde{M}_y \widetilde{M}_z^* + \widetilde{M}_y^* \widetilde{M}_z) \sin \theta \cos \theta$$

Magnetic SANS Theory



D. Honecker and A. Michels, Phys. Rev. B <u>87</u>, 224426 (2013); D. Mettus and A. Michels, J. Appl. Cryst. <u>48</u>, 1437 (2015); K.L. Metlov and A. Michels, Sci. Rep. <u>6</u>, 25055 (2016); A. Michels *et al.*, PRB <u>94</u>, 054424 (2016).

Micromagnetic Theory: balance of torques

[L. Landau and E. Lifschitz (1935); W.F. Brown Jr. (1940)]

$$E_{\rm tot} = \int_{V} \left(\epsilon_{\rm ex} + \epsilon_{\rm d} + \epsilon_{\rm ani} + \epsilon_{\rm dmi} \right) d^3 r$$



- Brown's equations of micromagnetics (Euler-Lagrange Eqs.) are a set of nonlinear partial differential equations with complex $\delta E_{\text{tot}} = 0$ boundary conditions
 - Numerical micromagnetics

$$(\mathbf{H}_{ex} + \mathbf{H}_{d} + \mathbf{H}_{ani} + \mathbf{H}_{dmi}) \times \mathbf{M} = 0$$
 exchange field magnetostatic field + Zeeman anisotropy field DMI field

> Necessary equilibrium condition

High-field limit: solution for Fourier coefficients

$$(\mathbf{H}_{\mathrm{ex}} + \mathbf{H}_{\mathrm{d}} + \mathbf{H}_{\mathrm{ani}} + \mathbf{H}_{\mathrm{dmi}}) \times \mathbf{M} = 0$$

based on (cubic symmetry)

$$\mathbf{H}_{\mathrm{dmi}} = -l_D \nabla \times \mathbf{M}$$

$$\widetilde{M}_{x} = \frac{p\left(\widetilde{H}_{p,x}\left[1 + p\frac{q_{y}^{2}}{q^{2}}\right] - M_{s}\widetilde{I}_{m}\frac{q_{x}q_{z}}{q^{2}}\left[1 + p\,l_{D}^{2}q^{2}\right] - \widetilde{H}_{p,y}p\frac{q_{x}q_{y}}{q^{2}} - i\left[M_{s}\widetilde{I}_{m}(1 + p)l_{D}q_{y} - \widetilde{H}_{p,y}p\,l_{D}q_{z}\right]\right)}{1 + p\frac{q_{x}^{2} + q_{y}^{2}}{q^{2}} - p^{2}l_{D}^{2}q_{z}^{2}}$$

$$\widetilde{M}_{y} = \frac{p\left(\widetilde{H}_{p,y}\left[1 + p\frac{q_{x}^{2}}{q^{2}}\right] - M_{s}\widetilde{I}_{m}\frac{q_{y}q_{z}}{q^{2}}\left[1 + pl_{D}^{2}q^{2}\right] - \widetilde{H}_{p,x}p\frac{q_{x}q_{y}}{q^{2}} + i\left[M_{s}\widetilde{I}_{m}(1 + p)l_{D}q_{x} - \widetilde{H}_{p,x}pl_{D}q_{z}\right]\right)}{1 + p\frac{q_{x}^{2} + q_{y}^{2}}{q^{2}} - p^{2}l_{D}^{2}q_{z}^{2}}$$



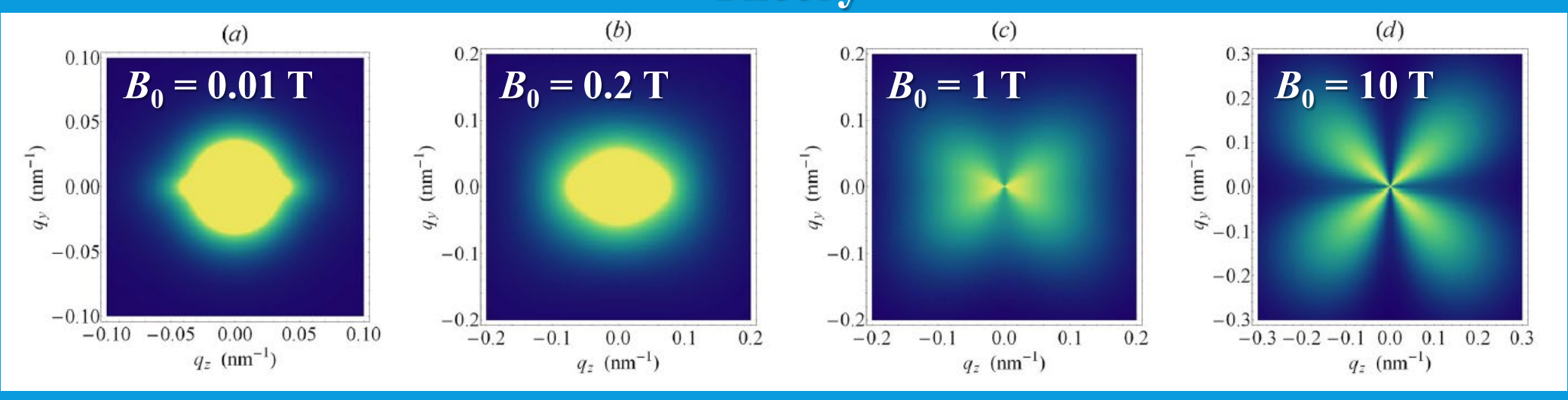
 $\mathbf{k}_0 \perp \mathbf{H}_0$

$$\frac{d\Sigma_{\text{mag}}}{d\Omega} \sim |\widetilde{M}_x|^2 + |\widetilde{M}_y|^2 \cos^2 \theta + |\widetilde{M}_z|^2 \sin^2 \theta - (\widetilde{M}_y \widetilde{M}_z^* + \widetilde{M}_y^* \widetilde{M}_z) \sin \theta \cos \theta$$

A. Michels *et al.*, PRB 94, 054424 (2016).
$$\widetilde{M}_{x,y,z} = \widetilde{M}_{x,y,z} (q, \theta, H, A, M_s, K, ...)$$

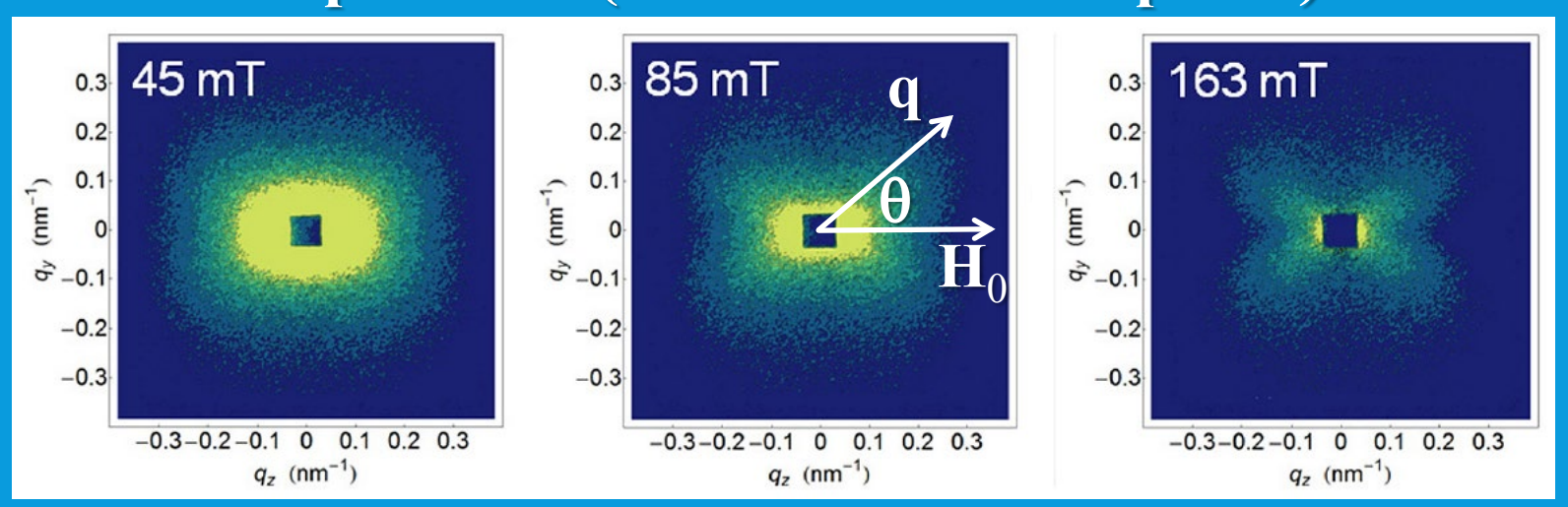
Analysis of magnetic SANS data

Angular Anisotropy of SANS pattern Theory



D. Honecker and A. Michels, PRB 87, 224426 (2013).

Experiment (Fe based nanocomposite)

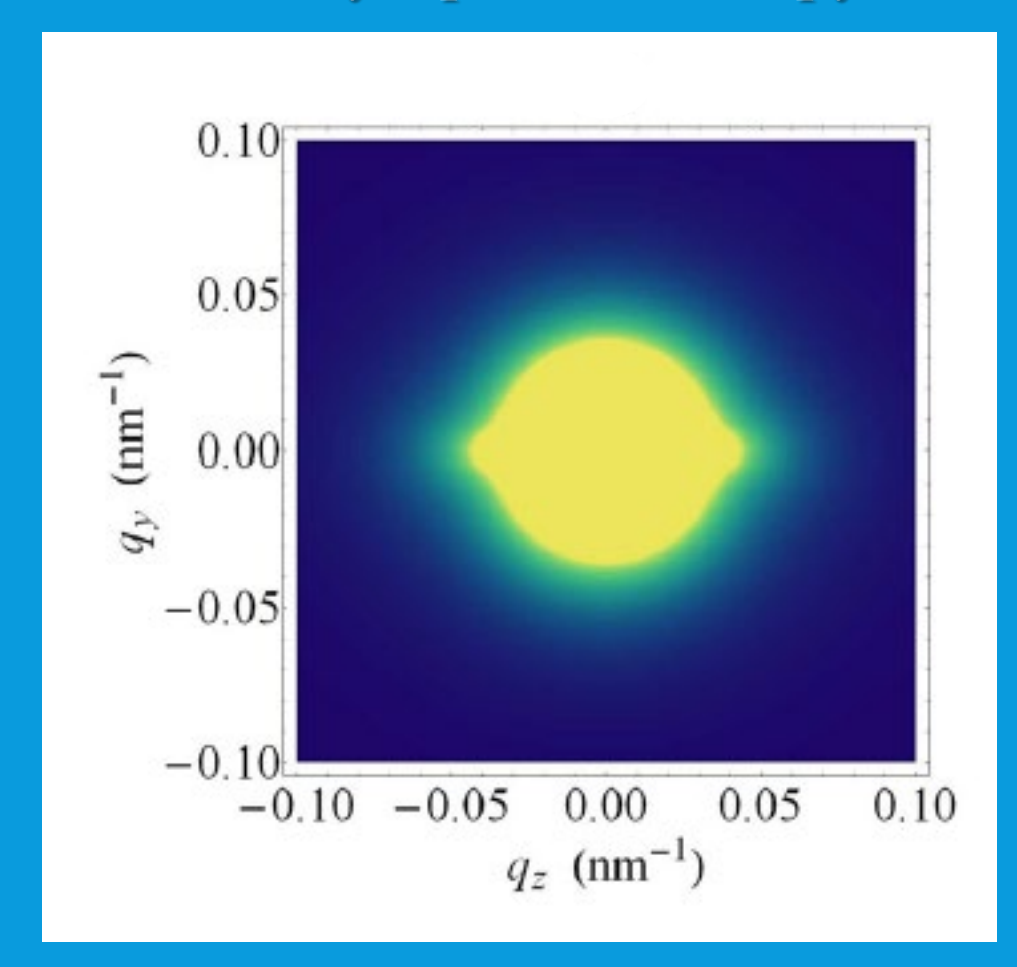


D. Honecker et al., PRB <u>88</u>, 094428 (2013).

Anisotropy of SANS pattern: flux-closure at nanoscale (due to $\nabla \cdot \mathbf{M} \rightarrow \mathbf{0}$)

Theory: spike anisotropy

Experiment (Nd-Fe-B)

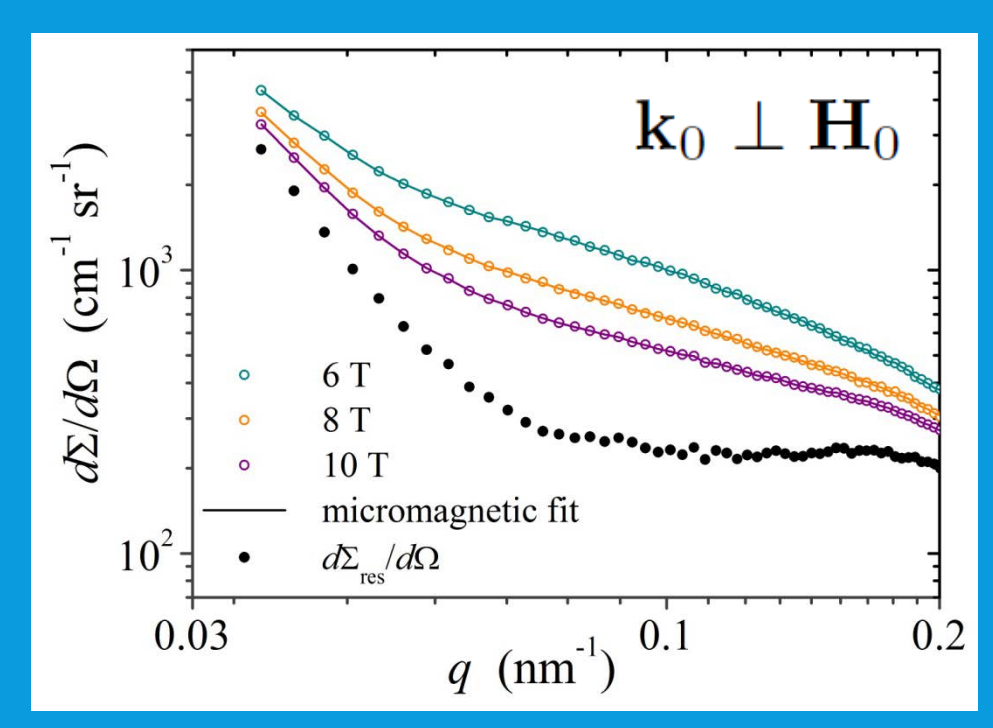


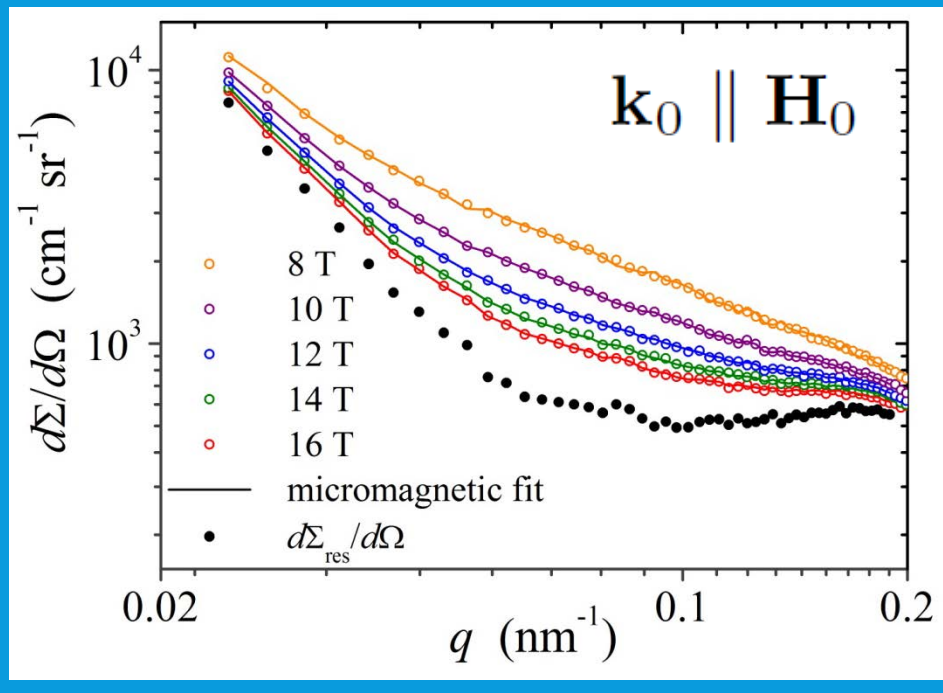
0.15 0.10 -0.05 q_{y} (nm⁻¹) 0.00 --0.05-0.10 --0.15-0.050.05 0.10 -0.15-0.100.00 $q_{z} (nm^{-1})$

D. Honecker and A .Michels, PRB <u>87</u>, 224426 (2013).

É.A. Périgo *et al.*, NJP <u>16</u>, 123031 (2014). M. Bersweiler *et al.*, PRB <u>108</u>, 094434 (2023).

Micromagnetic data analysis (Nd-Fe-B nanocomposite)





exchange-stiffness constant

$$A \cong 12.5 \times 10^{-12} \text{ J/m}$$

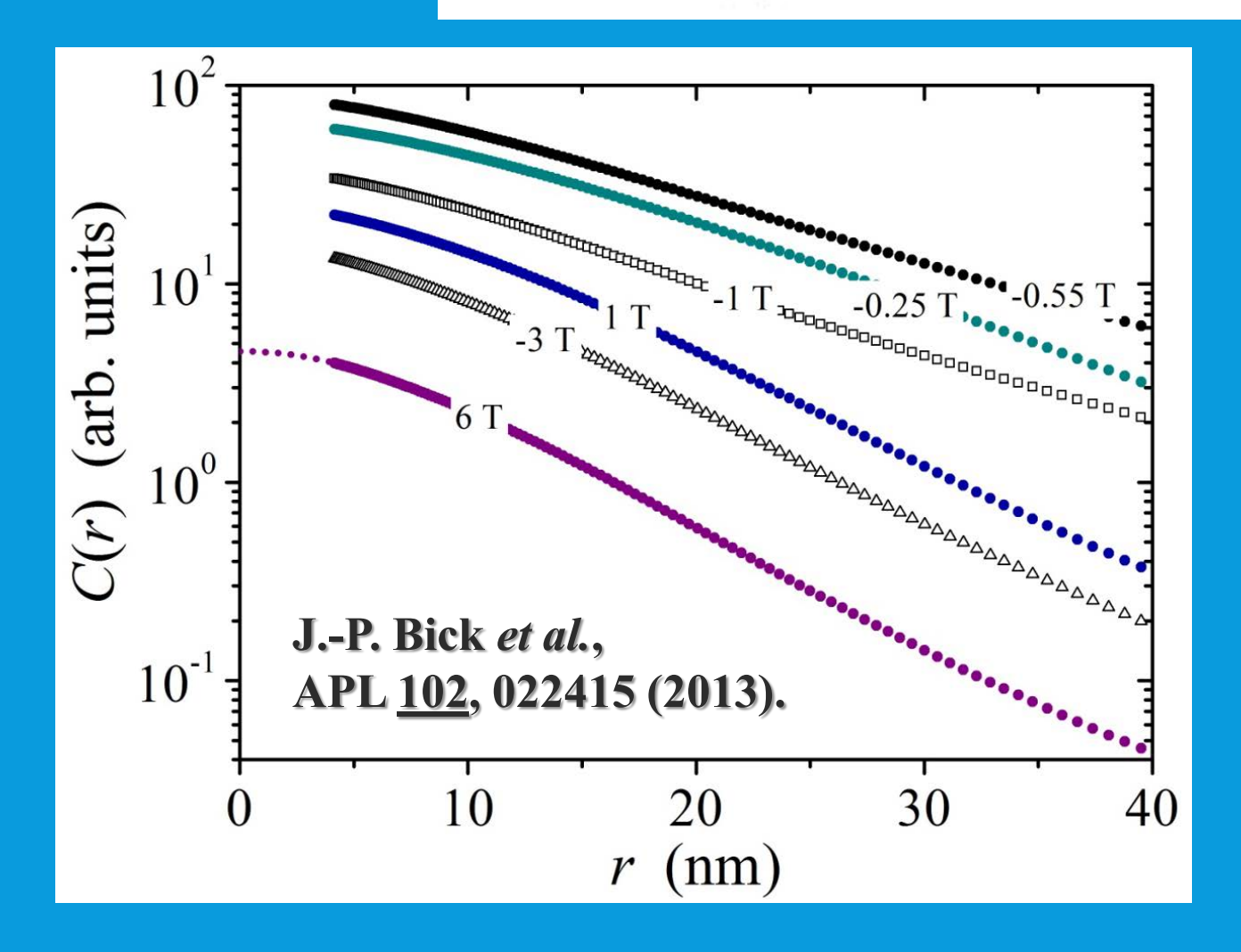
J.-P. Bick *et al.*, APL <u>102</u>, 022415 (2013). J.-P. Bick *et al.*, APL <u>103</u>, 122402 (2013).

plus information about

- magnetic anisotropy field
- magnetostatics
- correlation lengths
- ____

Real-space analysis: correlation function

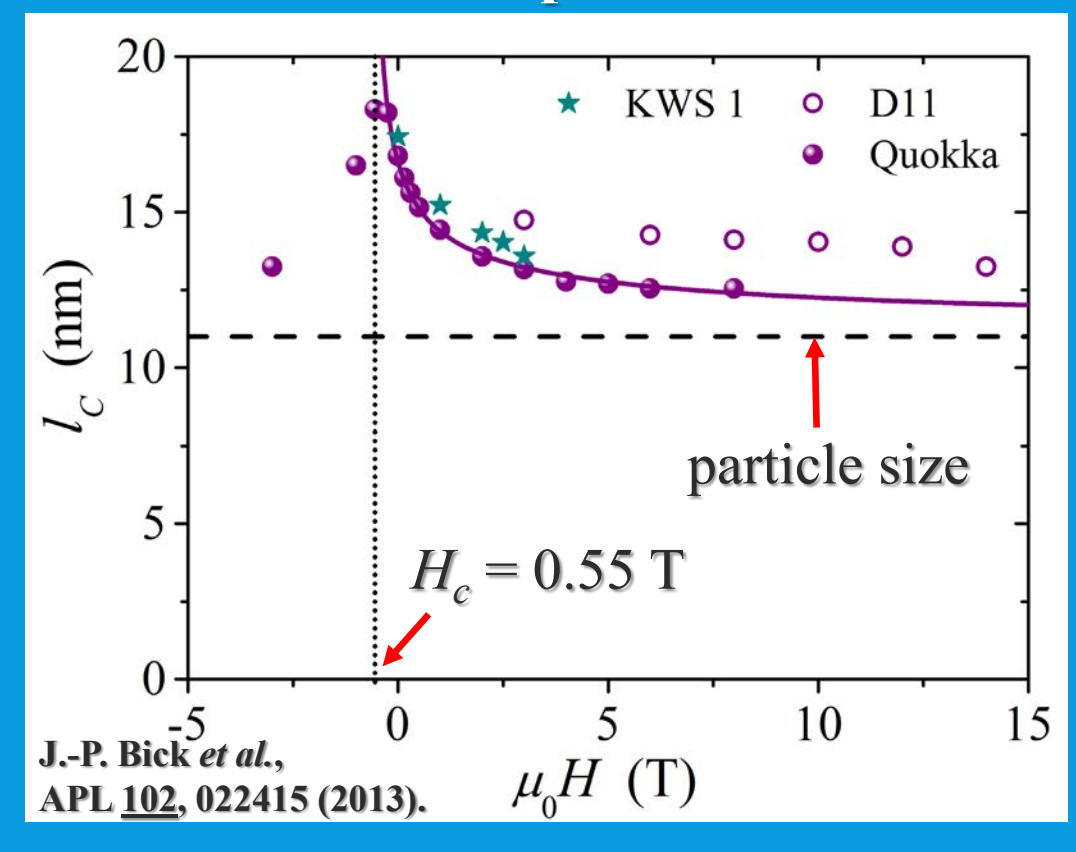
$$C(r) \propto \frac{1}{r} \int_0^\infty \frac{d\Sigma_M}{d\Omega}(q) \sin(qr) q dq$$



Nanomagnets exhibit non-exponential long-range decay of correlations

Magnetization reversal: Correlation length

Nd-Fe-B nanocomposite



micromagnetic model

$$l_C(H) = R + \sqrt{\frac{2A}{J_s(H + H^*)}}$$

 $R = \text{defect size (e.g., } R \cong \text{particle radius)}$ $H^* = \text{effective magnetic field}$ <u>Note:</u> for H = 0 and $H^* = H_K = 2K/J_s$

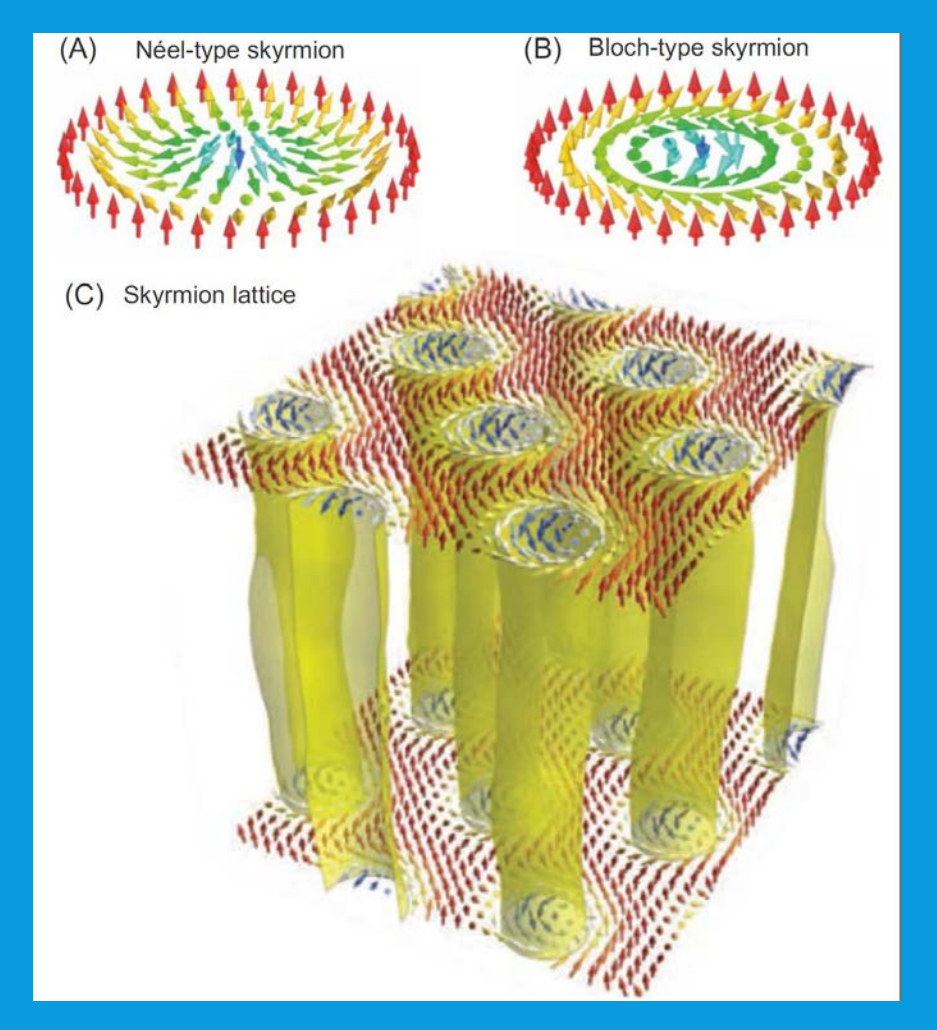
$$l_C(H) = R + \sqrt{\frac{A}{K}}$$

- \triangleright fit to data: R=10.9 nm and $\mu_0 H^*=0.60$ T
- The property at remainer at a state: penetration depth of spin disorder into $\operatorname{Fe_3B}$ phase $\Delta l_C = l_C(H) R \sim 5$ -6 nm

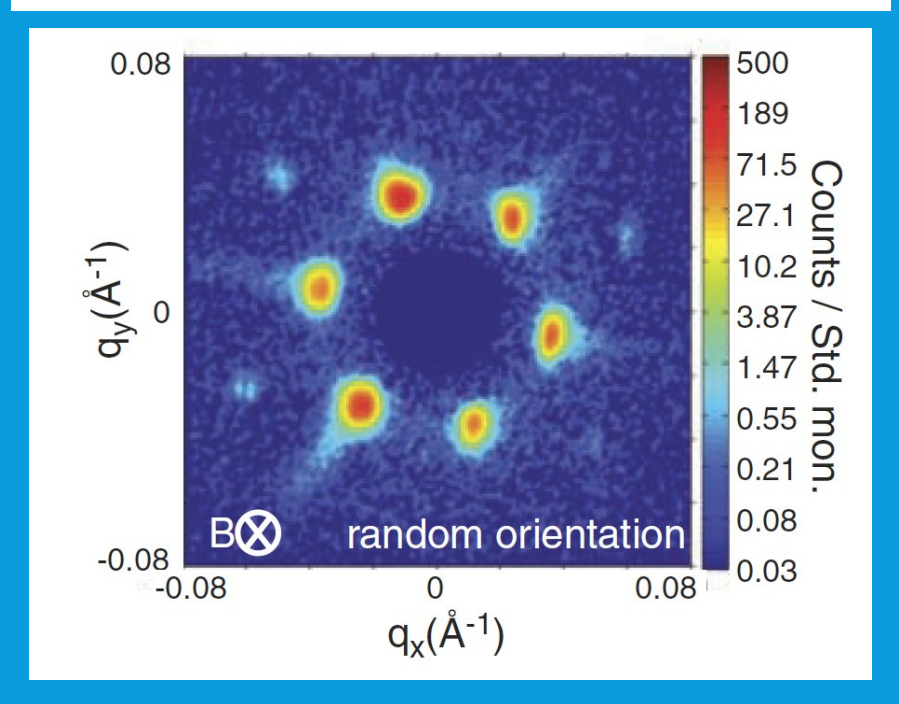
Selected Results

> Signature of DMI in magnetic SANS cross section?

DMI relevant in the context of skyrmion physics



$$H_{DMI} = \sum_{i,j} \mathbf{D}_{ij} \cdot (\mathbf{S}_i \times \mathbf{S}_j)$$



Mühlbauer, Pfleiderer et al., Science (2009).

- intrinsic DMI due to inversion-asymmetric crystal-field environment (MnSi, FeGe, Cu₂OSeO₃, Heusler-type alloys, ...)
- important for the stabilization of skyrmion lattices

Microstructural-defect-induced DMI

JOURNAL OF APPLIED PHYSICS

VOL. 34, NO. 4 (PART 2)

APRIL 1963

Dzialoshinski-Moriya Interactions About Defects in Antiferromagnetic and Ferromagnetic Materials

ANTHONY ARROTT

Scientific Laboratory, Ford Motor Company, Dearborn, Michigan

$$H_{DMI} = \sum_{i,j} \mathbf{D}_{ij} \cdot (\mathbf{S}_i \times \mathbf{S}_j)$$

- DMI is operative at defect sites due to the local breaking of structural inversion symmetry; relevant for disordered polycrystalline magnets and spin glasses (Fert and Levy, PRL 1980; Plakhty, Fedorov et al., PRB 2001; Grigoriev et al., PRL 2008)
- local chiral DMI couplings, present even in highly symmetric lattices

Defect-induced DMI: SANS Theory

$$\frac{d\Sigma^{\pm}}{d\Omega} \sim \frac{|\widetilde{N}|^2 + |\widetilde{M}_x|^2 + |\widetilde{M}_y|^2 \cos^2\theta + |\widetilde{M}_z|^2 \sin^2\theta - (\widetilde{M}_y \widetilde{M}_z^* + \widetilde{M}_y^* \widetilde{M}_z) \sin\theta \cos\theta}{\text{polarization-independent}}$$

$$\mp (\widetilde{N} \widetilde{M}_z^* + \widetilde{N}^* \widetilde{M}_z) \sin^2\theta \mp \imath \chi$$

polarization-dependent

$$\Delta \Sigma = \frac{d\Sigma^{-}}{d\Omega} - \frac{d\Sigma^{+}}{d\Omega} \sim 2(\widetilde{N}\widetilde{M}_{z}^{*} + \widetilde{N}^{*}\widetilde{M}_{z})\sin^{2}\theta + 2\imath\chi$$

Chiral function

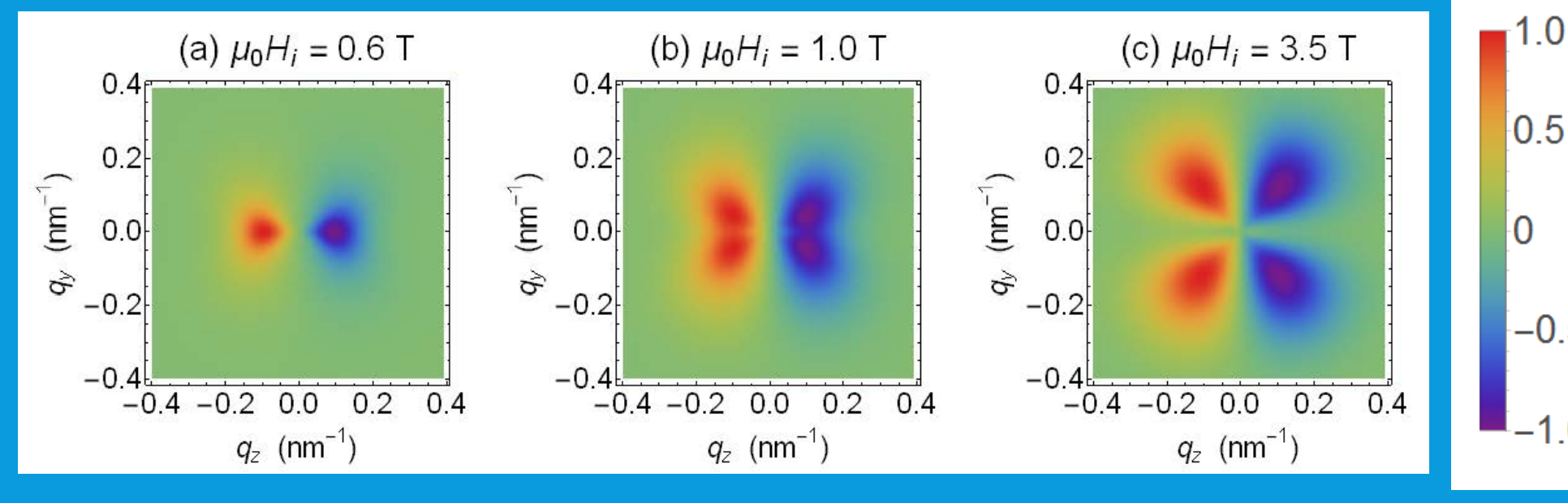
$$\chi(\mathbf{q}) = \left(\widetilde{M}_x \widetilde{M}_y^* - \widetilde{M}_x^* \widetilde{M}_y\right) \cos^2 \theta - \left(\widetilde{M}_x \widetilde{M}_z^* - \widetilde{M}_x^* \widetilde{M}_z\right) \sin \theta \cos \theta$$

Defect-induced DMI: SANS Theory

Chiral function

$$2i\chi(\mathbf{q}) = -\frac{2\widetilde{H}_p^2 p^3 \left(2 + p\sin^2\theta\right) l_D q\cos^3\theta + 4\widetilde{M}_z^2 p(1+p)^2 l_D q\sin^2\theta\cos\theta}{\left(1 + p\sin^2\theta - p^2 l_D^2 q^2\cos^2\theta\right)^2}$$

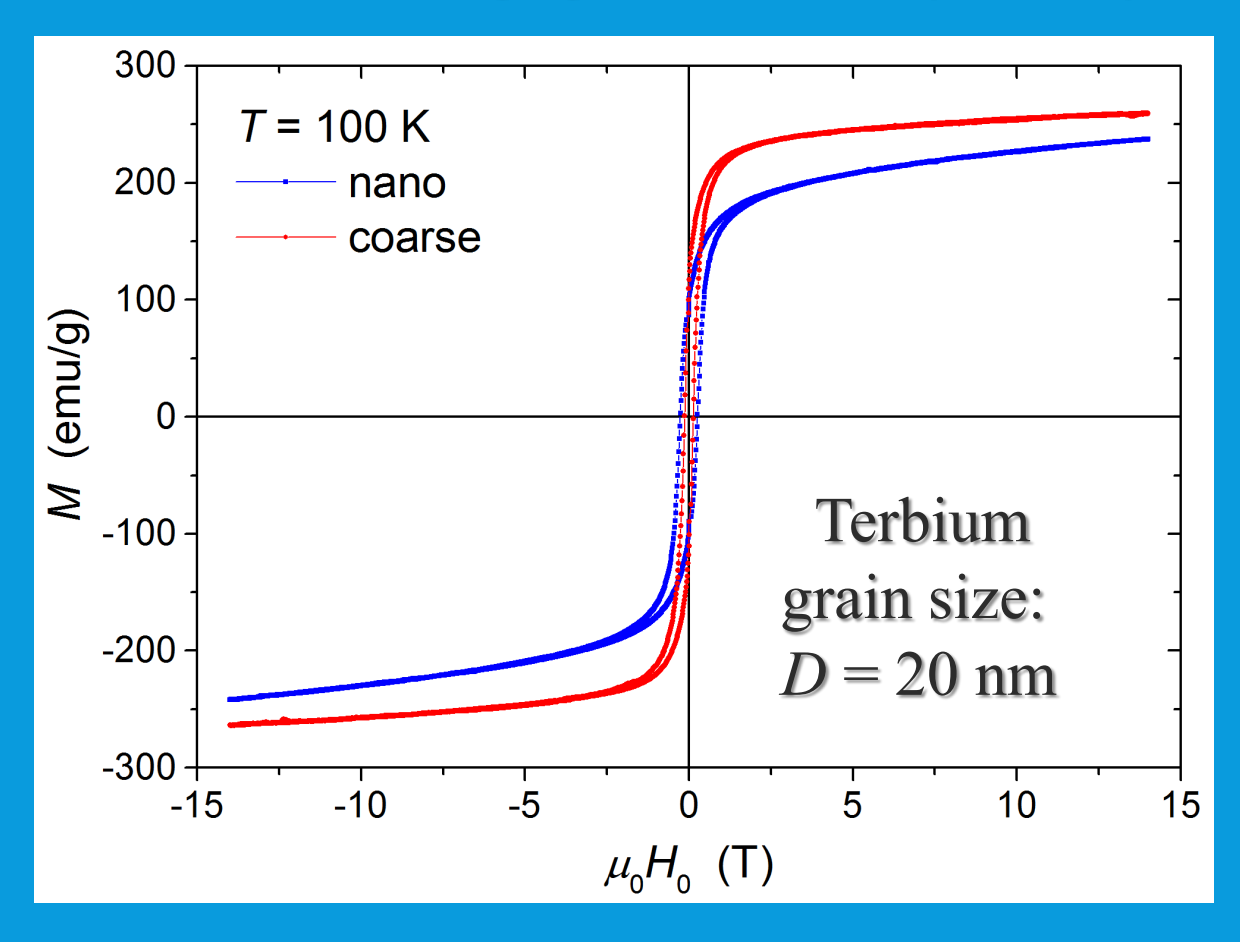
 $\widetilde{H}_p(\mathbf{q})$: Fourier transform of magnetic anisotropy field $H_p(\mathbf{r})$ $\widetilde{M}_s(\mathbf{q})$: Fourier transform of spatially-dependent local saturation magnetization $M_s(\mathbf{r})$



A. Michels et al., PRB <u>94</u>, 054424 (2016).

Defect-induced DMI in nanomagnets

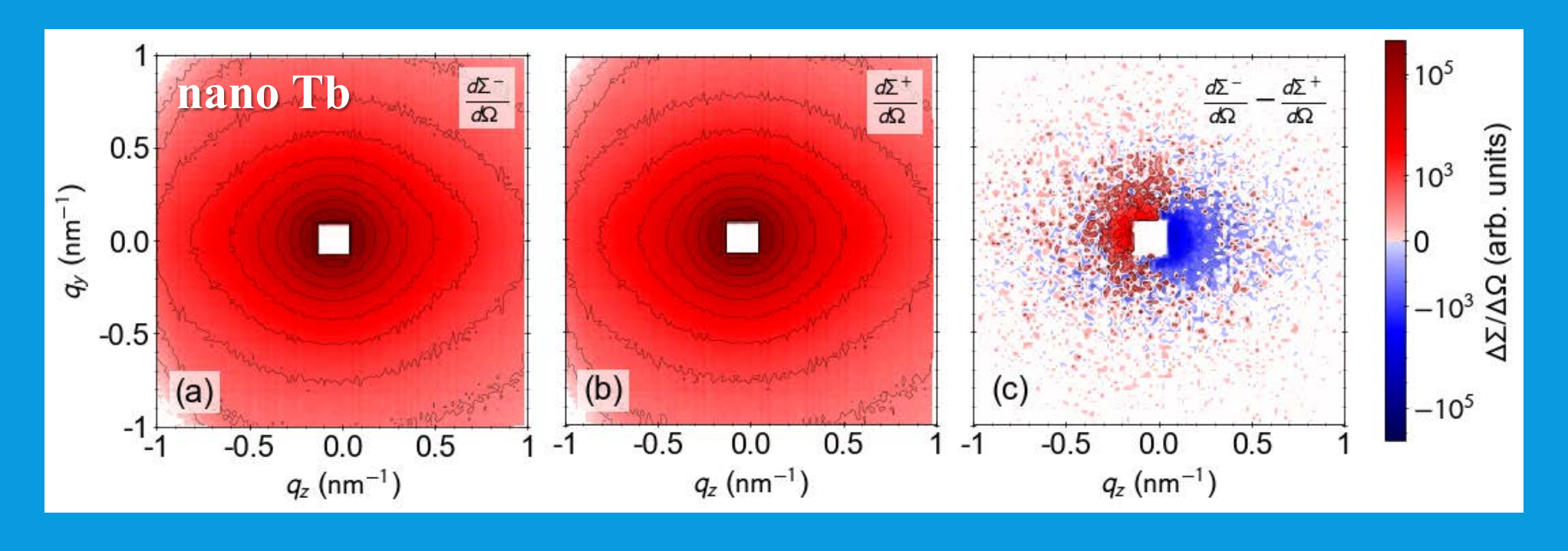
\Leftrightarrow Nanocrystalline Terbium (large grain-boundary density $\propto 1/D$)



> Defects (e.g., interfaces, dislocations) reduce magnetization

A. Michels et al., PRB 99, 014416 (2019).

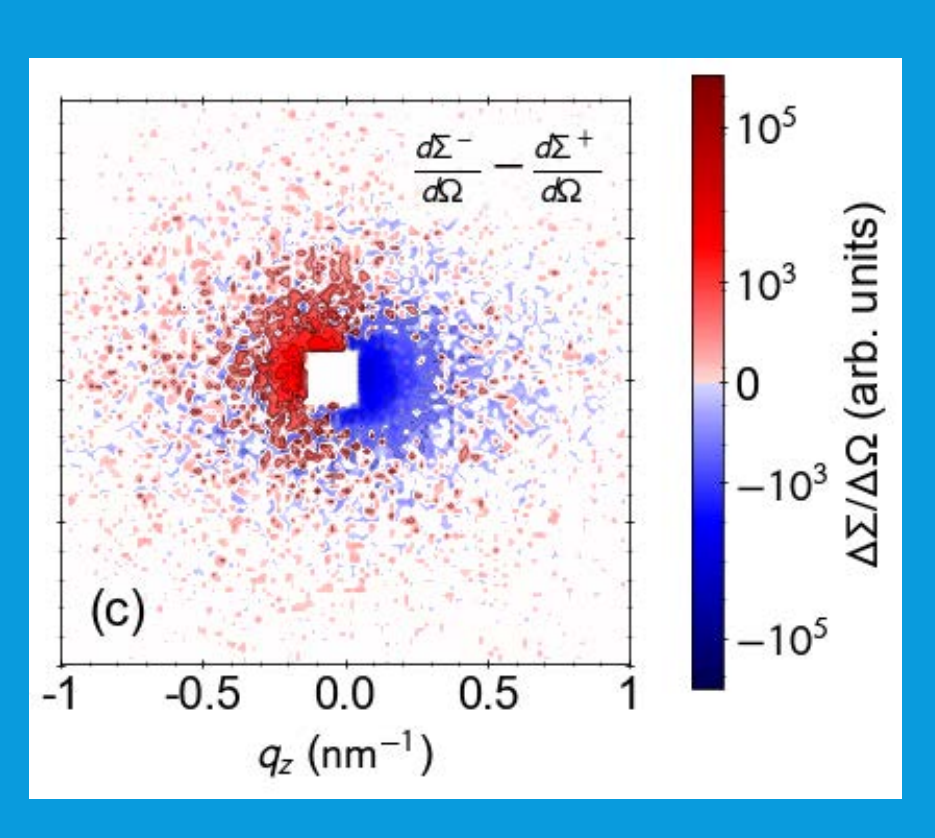
Defect-induced DMI: Experiment

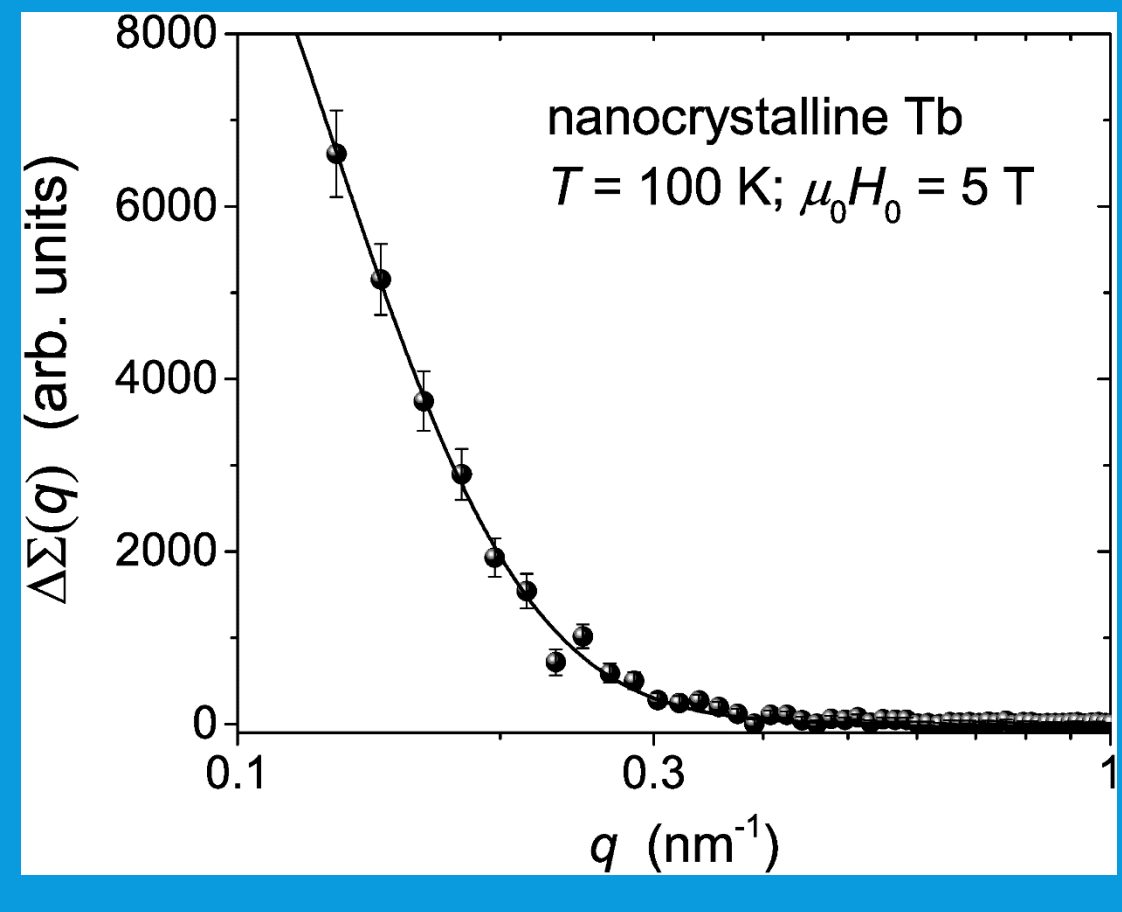


$$\Delta \Sigma = \frac{d\Sigma^{-}}{d\Omega} - \frac{d\Sigma^{+}}{d\Omega} \sim 2(\widetilde{N}\widetilde{M}_{z}^{*} + \widetilde{N}^{*}\widetilde{M}_{z})\sin^{2}\theta + 2\imath\chi$$

➤ Difference between "spin up" and "spin down" cross sections: only polarization-dependent terms survive

Defect-induced DMI: Experiment





average along horizontal direction

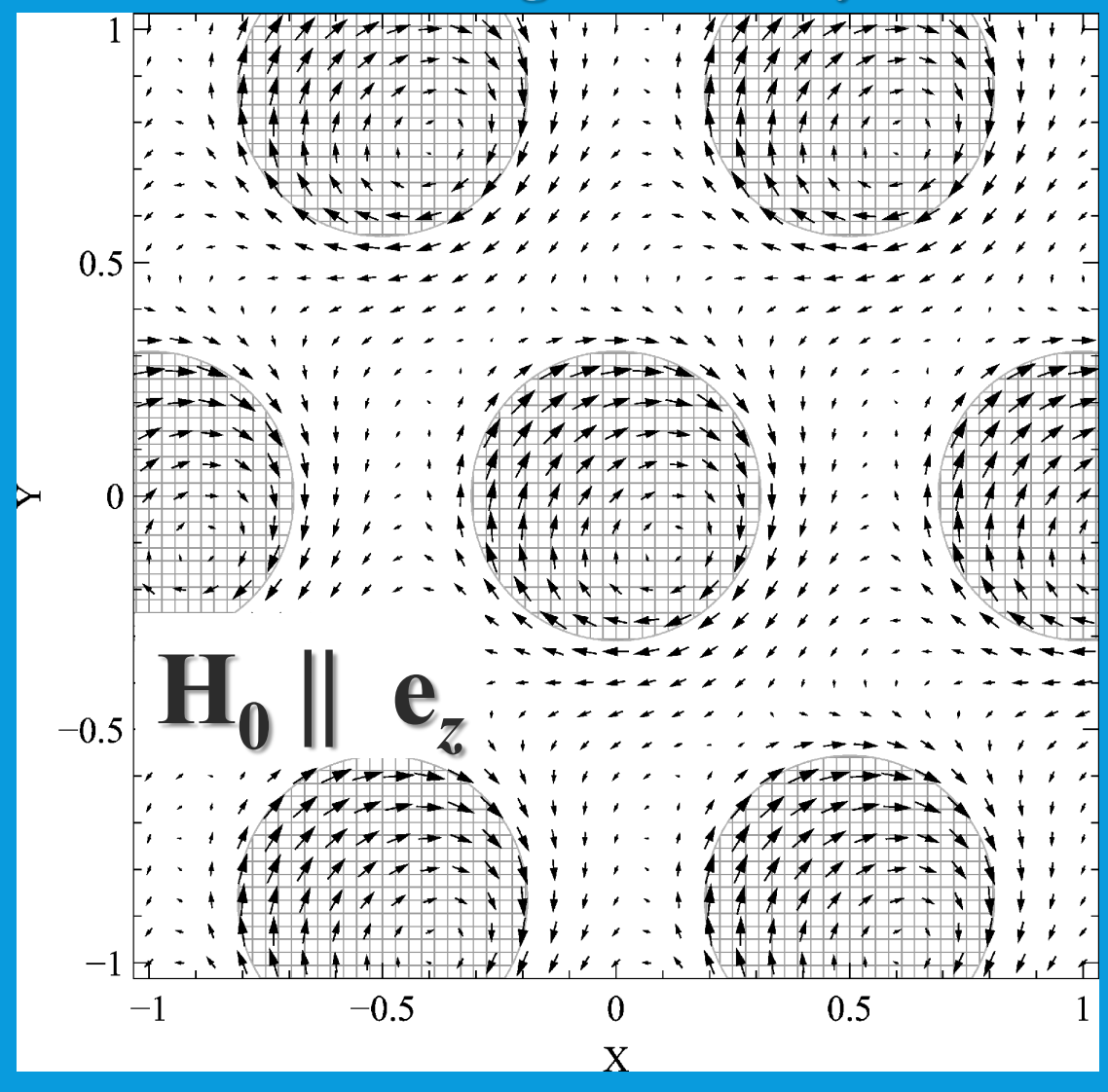
$$2i\chi(q, H_i) = \mp \frac{4\tilde{H}_p^2 p^3 l_D q}{(1 - p^2 l_D^2 q^2)^2}$$

 $D = 0.45 \pm 0.07 \text{ mJ/m}^2$

A. Michels et al., PRB 99, 014416 (2019).

Defect-induced DMI: Real-space structure

Result of micromagnetic theory

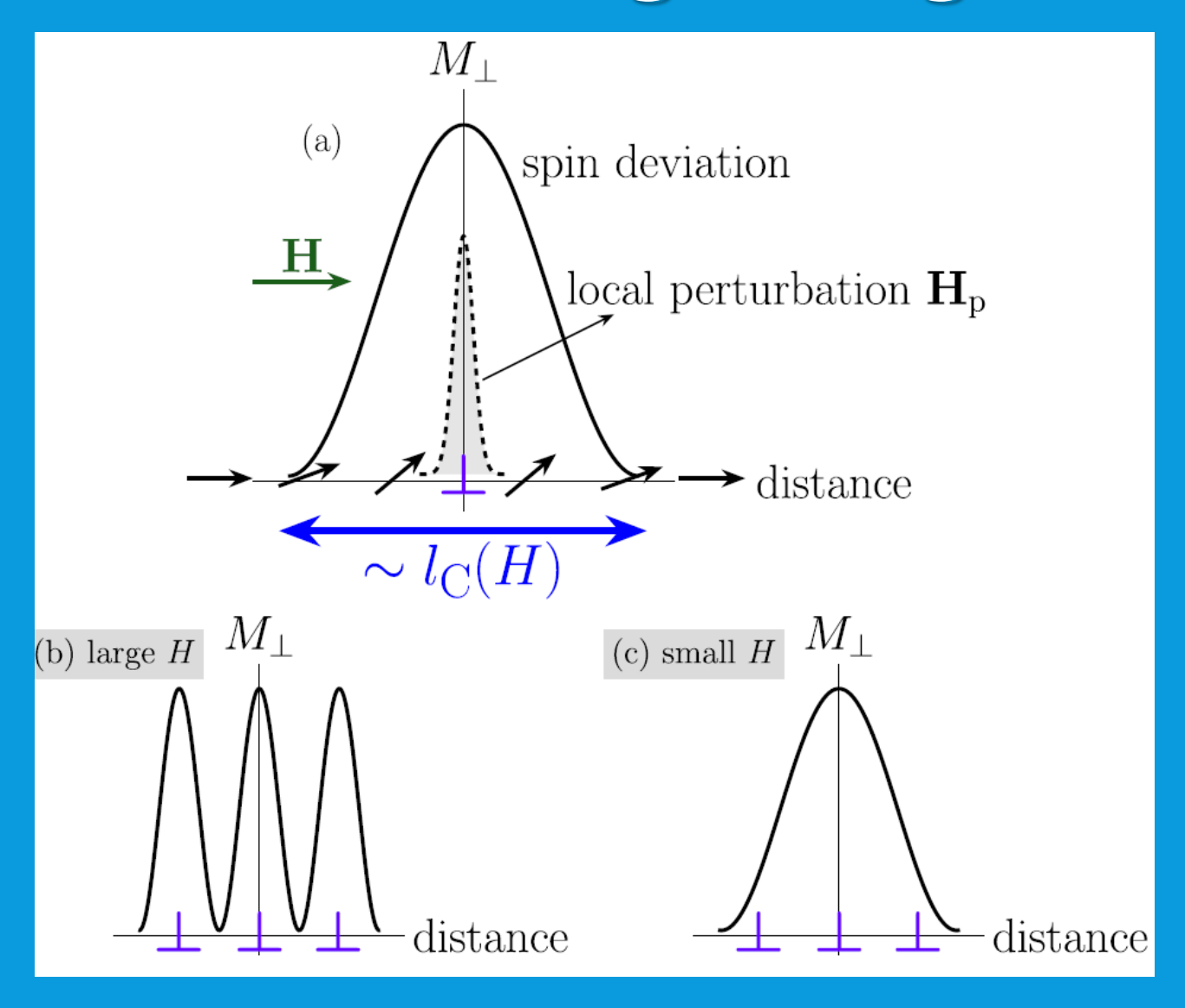


- Shaded circular areas:
 defect sites with different
 M_s and anisotropy field
- **M**(**r**) is asymmetric wrt the center of the defect
- Result of DMI, which introduces chiraltity into the sample
- Largest gradients in spin distribution near/at defect sites (interfaces)
- D-value from SANS
 experiment reflects
 emerging DMI strength
 at interfaces

A. Michels et al., PRB 99, 014416 (2019).

> Scaling in magnetic SANS

Scaling in magnetic SANS



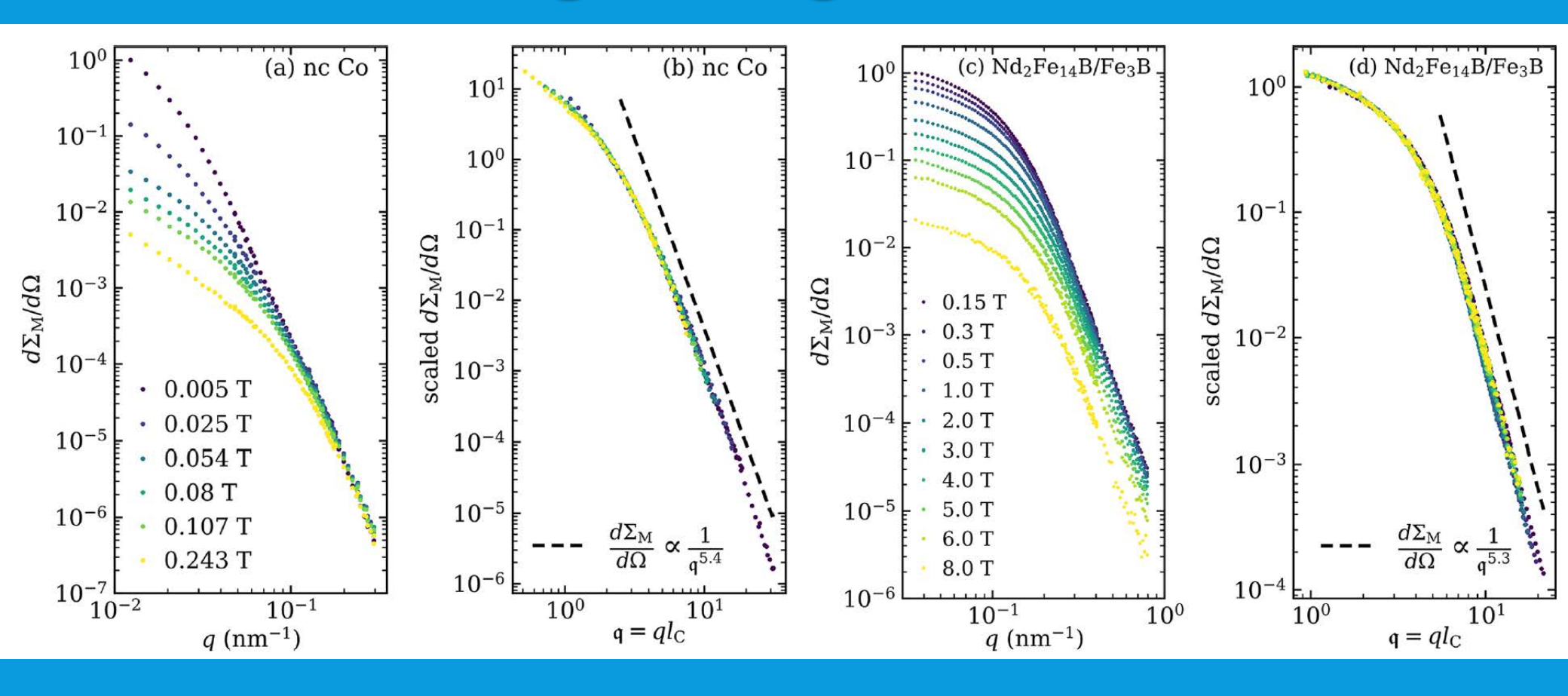
- $l_{\rm C}(H)$ is a measure for size of inhomogeneously magnetized regions around defects
- magnetization response similar at different fields *H*
- existence of scaling?
- Ansatz

defect size

$$l_{\mathrm{C}}(H) = D + l_{\mathrm{H}}(H)$$

exchange length
$$l_{\rm H}(H) = \sqrt{\frac{2A}{\mu_0 M_0 H}}$$

Scaling in magnetic SANS



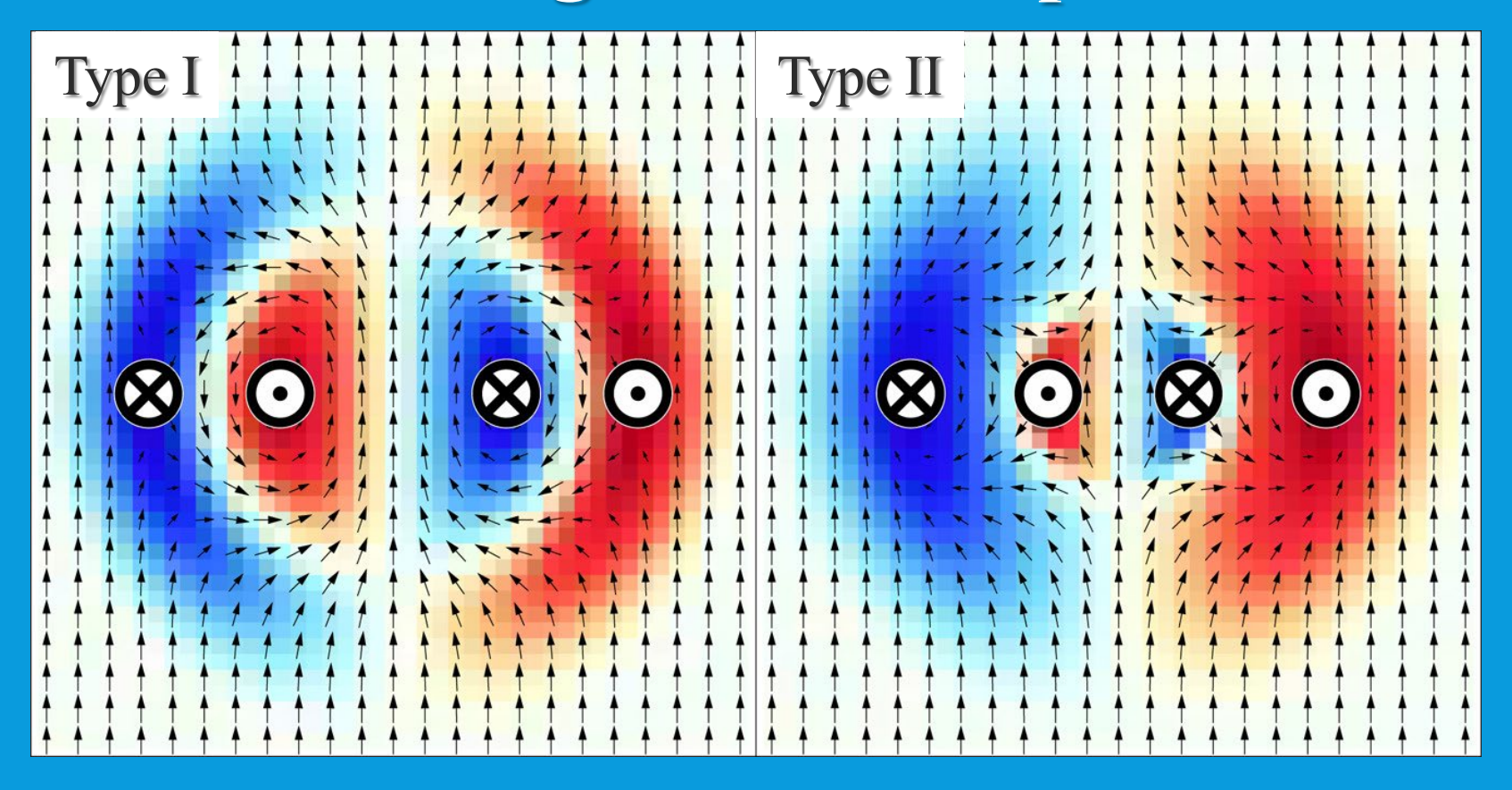
• horizontal scaling

$$q(H) = q l_{\mathbf{C}}(H)$$

□ *l*_C describes scaling behavior in the mesoscopic magnetic microstructure of bulk ferromagnets

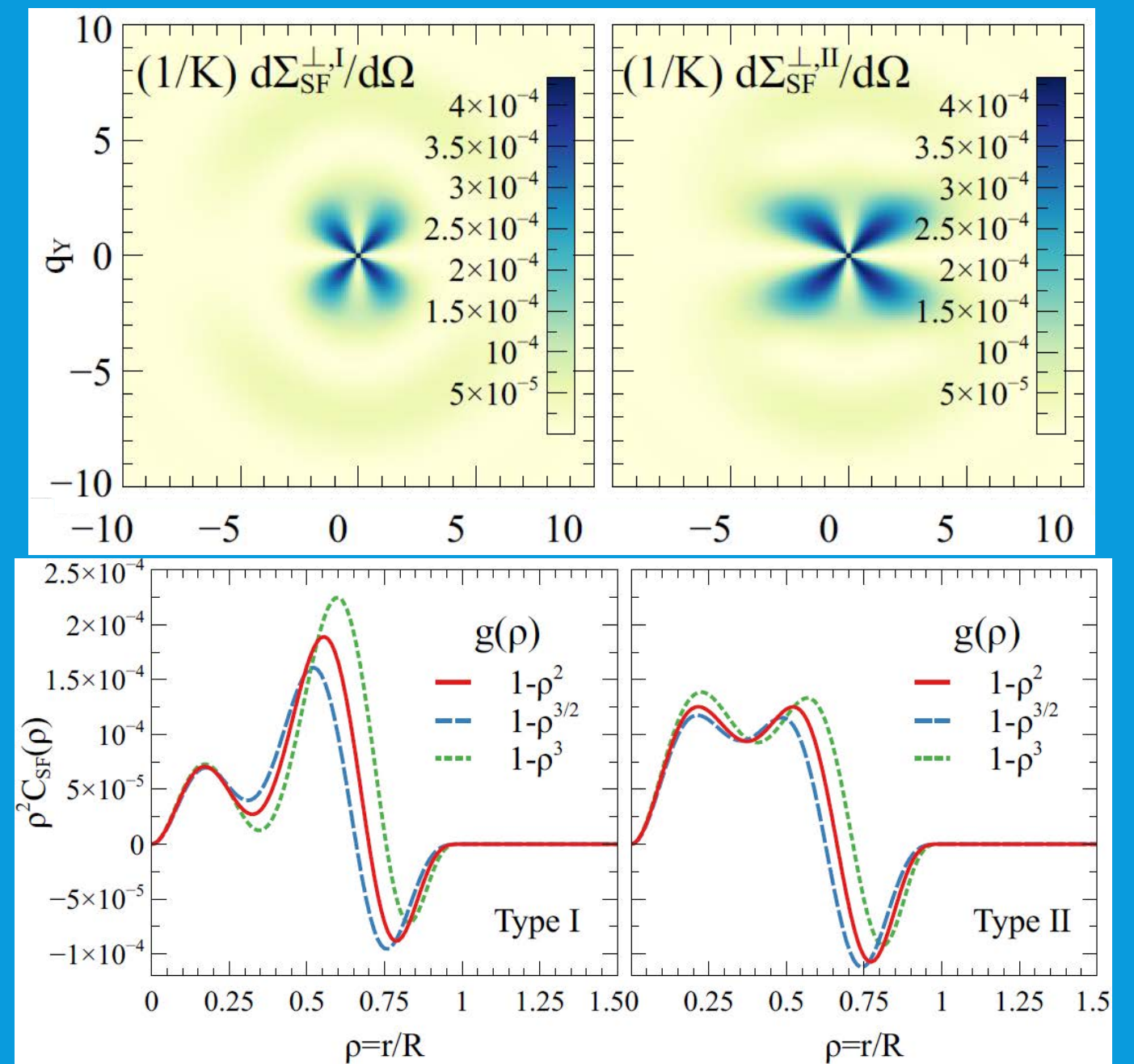
> Signatures of hopfions

SANS signature of hopfions



- Localized 3D topological object in an unbounded bulk magnet
- ❖ Contain a circular outer antivortex tube wrapped around a circular inner vortex tube (type I), and vice versa for type II

Spin-flip SANS and correlation function



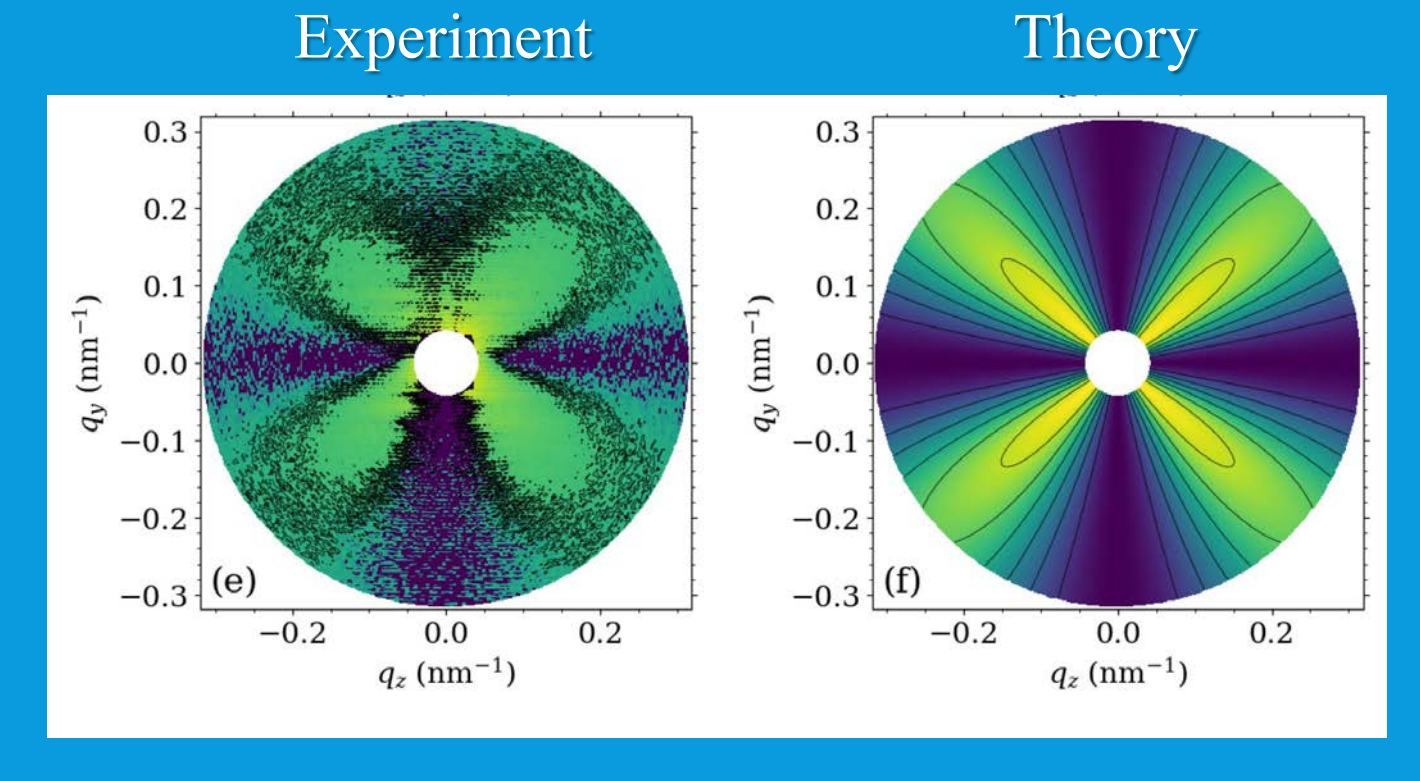
- Spin-flip SANS exhibits saturated-spheres-like scattering
- With a double-peak radial correlation function and a zero crossing produced by vortex and antivortex tubes
- Dipolar interaction
 destabilizes hopfions
 (MnSi is promising
 candidate material among
 skyrmion hosts)

K.L. Metlov and A. Michels, PRB <u>109</u>, L220408 (2024). K.L. Metlov, Physica B <u>695</u>, 416498 (2024).

Spin-disorder-induced anisotropy in polarized SANS

Difference between spin-up and spin-down SANS

$$\Delta \Sigma = K \left[(\widetilde{N} \widetilde{M}_z^* + \widetilde{N}^* \widetilde{M}_z) \sin^2 \theta \right]$$
$$-(\widetilde{N} \widetilde{M}_y^* + \widetilde{N}^* \widetilde{M}_y) \sin \theta \cos \theta$$



I. Titov et al., Phys. Rev. Lett. 135, 196706 (2025).

Conclusions

- ➤ Magnetic Neutron Scattering is important technique in physics and materials science to study <u>dynamics</u> and <u>structure</u> of magnetic materials
- Magnetic SANS in particular allows one to study <u>mesoscale</u> magnetization structure in the bulk of magnets (resolution range: ~ 1 nm- 20μ m)
- ➤ Magnetic SANS + micromagnetic theory is useful tool for <u>quantitative</u> analysis of bulk magnetic materials (exchange constant, magnetic anisotropy and magnetostatic fields, correlation length, ...)
- > Dipolar interaction results in angular anisotropies; must be taken into account for fundamental understanding of magnetic SANS
- > DMI in defect-rich materials results in asymmetry of polarized SANS; effect is generic to polycrystalline magnets
- **Existence of scaling; hopfion signatures**